ECM crosslinking enhances fibroblast growth and protects against matrix proteolysis in lung fibrosis.

Christopher J Philp[1], Ivonne Siebeke[1], Debbie Clements[1], Suzanne Miller[1], Anthony Habgood[1], Alison E John[1], Vidya Navaratnam[2], Richard B Hubbard[2], Gisli Jenkins[1] and Simon R Johnson[1]

[1]*Division of Respiratory Medicine, School of Medicine, University of Nottingham.*
[2]*Division of Epidemiology and Public Health, School of Medicine, University of Nottingham.*

 # Address correspondence to: Christopher J Philp; christopher.philp@nottingham.ac.uk;
Tel: +44 (0)115 8231069; fax: +44 (0)115 31059.

Running Head:
Matrix cross linking in IPF

Contributions:
Experimental work: CJP, IS, DC, SM, AH, AJ, VN
Conception and design of the study: CJP, GJ, SRJ
Analysis and interpretation: CJP, RBH, GJ, SRJ
Drafting the manuscript for important intellectual content: CJP, IS, AH, AJ, VN, RBH, GJ, SRJ

Acknowledgements
The study was funded by a Medical Research Council ~~n MRC DTC~~doctoral training studentship and the British Lung Foundation. The Trent lung fibrosis study was funded by the Medical Research Council. We are grateful to Christine Grainger-Boultby for technical assistance.

Abstract

Idiopathic pulmonary fibrosis (IPF) is characterised by accumulation of extra–cellular matrix (ECM) proteins and fibroblast proliferation. ECM cross-linking enzymes have been implicated in fibrotic diseases and we hypothesised that the ECM in IPF is abnormally cross-linked which enhances fibroblast growth and resistance to normal ECM turnover. We used a combination of *in vitro* ECM preparations and *in vivo* assays to examine the expression of cross-linking enzymes and the effect of their inhibitors on fibroblast growth and ECM turnover. Lysyl oxidase like 1, 2, 3 and 4 were expressed equally in control and IPF derived fibroblasts. Transglutaminase 2 was more strongly expressed in IPF fibroblasts. Lysyl oxidase like 2, transglutaminase 2 and transglutaminase generated cross-links were strongly expressed in IPF lung tissue. Fibroblasts grown on IPF ECM had higher LOXL3 protein expression and transglutaminase activity compared with those grown on control ECM. IPF derived ECM also enhanced fibroblast adhesion and proliferation compared with control ECM. Inhibition of lysyl oxidase and transglutaminse activity during ECM formation affected ECM structure as visualised by electron microscopy and reduced the enhanced fibroblast adhesion and proliferation of IPF ECM to control levels. Inhibition of transglutaminase, but not lysyl oxidase activity, enhanced the turnover of ECM *in vitro*. In bleomycin treated mice, during the post-inflammatory fibrotic phase, inhibition of transglutaminases was associated with a reduction in whole lung collagen. Our findings suggest that the ECM in IPF may enhance pathological cross-linking which contributes to increased fibroblast growth, resistance to normal ECM turnover to drive lung fibrosis.

Introduction

Idiopathic pulmonary fibrosis (IPF) is the most common idiopathic interstitial pneumonia with an incidence of 7.44 per 100 000 person-years and a prevalence which is rising year on year[1]. The lung architecture is progressively remodelled by the proliferation of fibroblasts, myofibroblasts and the deposition of extracellular matrix (ECM) leading to respiratory failure with a median survival of less than three years[2].

The deposition of fibrosis in IPF is heterogenous both in its spatial distribution and evolution over time. Regions of densely packed fibroblasts / myofibroblasts and ECM proteins, particularly collagen I, termed fibroblast foci, tend to be situated adjacent to less involved regions of the lung[3]. The activated myofibroblast is thought to be the main source of pathological ECM in IPF and present~~deposited both~~ in the fibroblast foci and the less densely involved areas of the lung[4]. The mammalian ECM consists of around 300 individual proteins which include the classical ECM proteins collagens, fibronectin, elastin, proteoglycans and glycoproteins, but also a large number of signaling molecules, post-translational modifying enzymes and proteases. The ECM is a dynamic and versatile part of the cellular environment influencing almost all cell functions, including proliferation and migration by binding to growth factors, by acting as a co-receptor for various ligands and signaling via endogenous growth factor domains or matricryptins generated by proteolytic processing[5 6]. Additionally, changes in the biomechanical properties of the ECM can induce gene expression programs affecting cell differentiation and function[7]. Consistent with its importance, multiple levels of regulation ensure tight control of ECM production, degradation, and remodeling[8]. However, in fibrotic diseases and cancers, abnormal ECM dynamics and organisation are major drivers of abnormal cell behaviour and ultimately organ failure[9].

In addition to ECM proteins, matrix degrading proteases, including matrix metalloproteinases (MMPs) -1 and -7, a disintegrin-like and metalloprotease with thrombospondin type 1 motif (ADAMTS)-14 and ADAMTS-5 are strongly overexpressed in IPF[10] suggesting the accumulation of ECM in IPF may not be

due to suppression of MMP activity as previously thought[11]. A potential explanation for the increase in both ECM proteins and proteases is that the ECM in IPF may be abnormally resistant to ECM degrading proteases. Stabilisation of the ECM by cross linking of collagen/fibronectin by transglutaminase 2 (TG2)[12] and collagen/elastin by lysyl oxidase like 2 (LOXL2)[13] respectively, can protect ECM from proteolysis in other organs[14,15].

TG2 is an 80 kDa protein with a number of enzymatic and non-enzymatic functions. TG2 cross-links the ECM by calcium dependent transamidation / deamidation of the glutamine or lysine side chains of many proteins resulting in lysine crosslink formation. LOXL2 is a member of the lysyl oxidase gene family, which share conserved C-terminal copper binding and catalytic domains, and act as extracellular copper-dependent amine oxidases that deaminate the lysine ε-amino group to cross-linkage collagen and elastin monomers[16]. Both TG2 and LOXL2 are overexpressed in IPF and their inhibition or absence during the induction of fibrosis reduces lung inflammation and fibrosis in bleomycin treated animals[12,13]. Here, we will test the ~~hypothesis~~ hypotheses that the ECM in IPF is aberrantly cross-linked, supports fibroblast growth, ~~and~~ confers resistance against ECM turnover by proteolysis and that inhibition of ECM cross-linking can affect these processes.

Methods

Full details of all methods and supporting data are provided in the online supplement.

Cells, tissues and serum samples

IPF derived fibroblasts were obtained from patients undergoing lung biopsy for the diagnosis of interstitial lung disease. Control fibroblasts were obtained from patients undergoing lung tumor resections from uninvolved areas of the specimen. Cells were cultured in DMEM containing 10% foetal bovine serum and characterised by immuno-staining for α-SMA, S100A4 and fibroblast activation protein (supplementary figure 1). IPF and control lung tissue was obtained from The Nottingham Health

Science Biobank. IPF and control serum with linked clinical data were obtained from the Trent Lung Fibrosis study which has been described previously[17]. The use of cells, tissues and serum was approved by the Nottingham Research Ethics committee and all patients provided written informed consent.

ECM preparations and assays

ECM was obtained from three IPF derived and three control fibroblast cultures as described[18]. ECM protein was analysed in two fractions, that soluble in RIPA buffer (soluble fraction) and that isolated by physical scraping and solubilsation in an 8M urea based buffer (insoluble fraction). ECM structure was visualized by electron microscopy using a Jeol 6060LV scanning electron microscope (Jeol ltd. UK). For ECM degradation assays, fibroblasts were incubated with 1µC/ml tritiated proline during matrix deposition. Tritiated proline labelled ECM preparations were digested with recombinant MMPs -1, -2 and -7 (R&D Systems, UK) and tritium measured in the soluble fraction by scintillation counting and expressed as disintegrations per minute (DPM) as a marker of ECM proteolysis. The effect of ECM stiffness on TG2 activity was analysed by culturing control fibroblasts on ~~tissue culture plates~~substrates of variable stiffness (SoftSubstrates, CA, USA). *In vitro* TG2 cross-linking was performed by incubation of recombinant human TG2 protein (500 ng/ml) or controls with 50ug/ml collagen type 1 (Advanced Biomatrix, USA) and 50ug/ml fibronectin (Sigma Aldrich, UK) overnight at 37 °c on a rotating shaker.

***In vitro* cell proliferation, adhesion and apoptosis assays**

Fibroblasts were cultured on ECM preparations for 48 hours and cell growth/proliferation determined by MTT reduction assay, ~~and~~ 5-ethynyl-2'-deoxyuridine (EdU) DNA incorporation and cell counting as described[19]. For adhesion assays, fluorescently labelled control fibroblasts were seeded onto ECM preparations and adherent cells measured by average well fluorescence after two hours. Apoptosis was assessed using an In Situ Cell Death Detection kit, AP (Roche Diagnostics, UK).

Formatted: Font color: Text 1

Formatted: Font color: Text 1

Cross-linking enzyme analysis

Gene expression for LOX, LOXL1, 2, 3, 4 and TG2 in IPF derived and control fibroblasts grown on IPF and control matrix were measured by real time RT-PCR using β-actin as the reference gene as described in the supplement. TG2 and LOXL3 protein were measured by ELISA (CusaBio Biotech Co. Ltd, MD, USA and Cloud Clone Corp., TX, USA.). Transglutaminase activity was determined using the Transglutaminase Assay Kit (Sigma Aldrich) and LOX activity by a Fluorometric Lysyl Oxidase Activity Assay Kit (Abcam, Cambridge UK). Immunohistochemistry was performed as described [20].

Bleomycin model of fibrosis

Six to eight week old C57BL/6 mice received 60 IU of intra-tracheal bleomycin as described[21]. At either 14, 24 or 34 days later, intraperitoneal cystamine (100mg/kg) was administered daily for ten days. Mice were then sacrificed by terminal anesthesia, blood samples taken, the lungs excised and snap frozen. Total lung collagen was assessed by hydroxyproline assay as described[22]. Animal work was approved by the Animal Welfare and Ethical Review Board of the University of Nottingham. Full details are provided in the on-line supplement.

Results

Expression of ECM cross-linking enzymes in fibroblasts, lung tissue and serum

We examined the expression of the LOX and transglutaminase family enzymes in control and IPF derived fibroblasts cultured on tissue culture plastic by quantitative, real time RT-PCR. *LOXL1-4* mRNAs were detected in all cells with expression not significantly different between control and IPF derived fibroblasts. The *LOX* transcript was also present in all cells but at very low levels. The TG2 transcript (*TGM2*) was expressed in normal fibroblasts and over 70 fold more strongly in IPF derived fibroblasts; (control 2.90 vs. IPF 177.5. n=3, $P<0.05$). Transglutaminase 6 and 7 transcripts were not present in either cell type (Figure 1). Total ECM protein, total collagen, collagen synthesis (supplementary figure 2) and collagen isoform gene expression did not vary between IPF and control fibroblast ECM (supplementary figure 3).

We then examined cross-linking enzymes, N-epsilon γ-glutamyl lysine cross-links, α-smooth muscle actin, collagen, using picro-sirius red and the proliferation marker ki67 in lung tissue from three control and eight patients with IPF. TG2 and N-epsilon γ-glutamyl lysine cross-links are present in control alveolar epithelium and strongly expressed in all areas of IPF tissue. Immunostaining for TG2, and the TG2 cross-link was ubiquitous in all areas of IPF tissue, including those with dense fibrosis, regions less involved by fibrosis and fibroblast foci. TG2 and its associated cross-link paralleled the deposition of collagen and αSMA in lung tissue. P~~In general p~~roliferating cells identified by ki67 positivity were ~~also~~ present in all areas of IPF tissue (figure 2). Within areas of dense fibrosis and fibroblast foci, proliferating cells tended to have fibroblast morphology whereas in areas of lesser fibrosis, had a morphology consistent with inflammatory cells. ~~LOXL3 was not expressed in normal lung tissue.~~ LOXL2 was ~~also~~ expressed in control and IPF tissue. LOXL3 was not expressed in normal lung tissue and was present at low level~~There was weak staining for LOXL3~~ in IPF tissue although positive control tissue (small intestine, not shown) stained more strongly (supplementary figure 4).

To determine the systemic expression of these cross-linking enzymes in patients with IPF we studied levels of circulating LOXL3 and TG2 in 60 patients with IPF, 30 of whom had died within a year of recruitment, 30 who had survived for more than one year and 30 age and sex matched controls. There were no significant differences, for either LOXL3 or TG2, between those with IPF and age matched controls. For all 60 with IPF, there was no association between serum LOXL3 or TG2 and FVC. Similarly, there was no difference between serum LOXL3 or TG2 levels between patients who were alive or who had died (supplementary figure 7~~5~~).

IPF matrix induces LOXL3 and TG2 expression

We hypothesized that ECM derived from IPF fibroblasts may promote its own cross linking. To test this we produced ECM from fibroblasts derived from three control and three patients with IPF. All six cell types were seeded onto each matrix type and cross linking gene expression examined by quantitative, real time RT-PCR. *LOXL3* was strongly induced in both cell types when grown on IPF derived ECM with the matrix type accounting for 75.5% of total variation (P<0.001. Figure 3a). TG2 mRNA showed a trend towards increased expression in IPF derived fibroblasts over control cells independent of matrix substrate, however this was not significant. Other cross-linking enzymes did not vary with cell or ECM type.

T~~G~~ransglutaminase activity and LOXL3 protein were measured in supernatants from these cultures. ~~TG2~~ Transglutaminase activity in supernatants increased in a cell dependent manner. ~~in~~ IPF fibroblasts on control matrix ~~showed~~had increased TG2 activity over control ~~derived~~ cells on control matrix (control 0.22AU vs. IPF 0.36AU. n=3, P<0.05). In addition, ~~, whereas~~ TG2 activity increased ~~by~~ 2 fold when control fibroblasts were seeded onto IPF ECM when compared with control matrix (control 0.22AU vs. IPF 0.42AU. n=3, P<0.01. Figure 3b and supplementary figure 5). Consistent with the gene expression data, LOXL3 protein expression was up regulated 3.3 fold in control fibroblasts grown on IPF compared with control matrix (control 280.4pg/ml vs. IPF 922.9pg/ml. n=3, P<0.001) and 4.2 fold in IPF fibroblasts grown

on IPF compared with control matrix (control 248.9pg/ml vs. IPF 1053pg/ml, n=3, *P*<0.001. Figure 3c). To determine if the observed changes were due to enhanced ECM stiffness we examined the transglutaminase activity of fibroblasts grown on substrates with a Young's modulus varying between 0.5-64 kPa and found that ECM stiffness had no effect on transglutaminase activity (Supplementary figure 8~~6~~).

IPF matrix enhances fibroblast adhesion and proliferation

To determine whether IPF derived ECM contributes to an environment which supports expansion of the fibroblast population we examined adhesion, proliferation and resistance to apoptosis of fibroblasts on control and IPF derived ECM. IPF derived ECM enhanced control and IPF derived fibroblast adhesion by 2.4 (*P<0.05*) and 7.5 fold (*P<0.01*) respectively over control ECM (Figure 4a). In the absence of a mitogen, MTT reduction and DNA synthesis did not differ when cultured on IPF and control derived ECM for 48 hours. Stimulating growth with either 1% foetal bovine serum or PDGF-bb (5ng/ml) enhanced control fibroblast ~~growthand metabolic activity~~MTT reduction on IPF derived ECM by 26 (*P*<0.0001) and 17 (*P*<0.01) fold respectively ~~(Figure 4b) . Furthermore, IPF ECM enhanced~~ and DNA synthesis, as measured by EdU incorporation by ~~xx~~1.2~~2.4 in the presence of either FBS or PDGF-bb~~ (*P*<0.01) ~~&~~and ~~xx~~2.~~1~~1.2 fold (*P*<0.05) respectively (Figure 4b). ~~In the absence of a mitogen, fibroblast number did not differ when~~ staurosporine or ~~f~~Fas ligand as judged by DNA fragmentation, caspase 3 or ~~parp~~ PARP cleavage (supplementary figure 6~~7~~).

Enhanced adhesion and proliferation on IPF derived ECM is dependent on matrix cross-linking

We then examined if the functional effects of IPF derived ECM were a consequence of ECM cross-linking. ECM preparations were produced by cells treated with inhibitors of TG2 (cystamine dihydrochloride) and the LOX family (beta amino-proprionitrile, βAPN). Treatment of cells with these inhibitors had no effect on the amount of ECM deposition nor cell viability (data not shown). To determine whether cystamine and βAPN affected ECM structure; we examined the ECM deposited by both cell types and

Formatted: Font: Italic

Commented [SJ1]: Add fold change for both for consistency

Commented [PC2R1]:

Formatted: Not Highlight

Formatted: Font: Italic

the effect of the cross-link inhibitors using scanning electron microscopy. Both cystamine and βAPN disrupted the ordered ECM fibrillary structure (figure 5a). The enhanced fibroblast adhesion on IPF derived ECM was reduced to a similar level to that of control ECM by both cystamine (vehicle = 334.0 AU vs. cystamine = 283.2 AU, $P < 0.0001$, n=3) and βAPN (vehicle = 334.0 AU vs. βAPN =254.2 AU, $P<0.0001$, n=3. Figure 5b). Enhanced fibroblast proliferation was reduced 6.5 fold by cystamine treatment of IPF ECM (vehicle = 0.478 AU vs. cystamine = 0.073 AU, $P < 0.01$, n=3). Cystamine treatment of control ECM resulted in a paradoxical increase in MTT reduction in control cells ~~but not control derived ECM~~. βAPN inhibited proliferation on IPF ECM in a similar manner to cystamine by 3.4 fold (vehicle = 0.478 AU vs. βAPN = 0.139 AU, $P<0.05$, n=3. Figure 5c).

To ensure these observations were not due to a non-specific effect of cystamine, we first examined LOX activity in cystamine treated cells and found no effect of cystamine on LOX cross-linking activity (data not shown). We next performed fibroblast adhesion and proliferation assays on *in vitro* cross-linked collagen / fibronectin coated plates which had been incubated with either vehicle control, recombinant TG2 (500 ng/ml) or TG2 and cystamine. Adhesion of MRC5 fibroblasts to this ECM coating was enhanced 2.1 fold (P ~~<~~<0.05) by TG2 treatment. Co-incubation with cystamine completely abrogated the increased adhesion (figure 5d). Cell number in response to 1% serum over 72 hours was enhanced 1.4 fold (P ~~<~~< 0.05) by TG2 treatment and the increase blocked by cystamine (figure 5e).

We then examined the co-localisation of the TG2 associated cross-link and proliferating cells identified by ki67 staining, in eight IPF lung samples. Both the cross-link and ki67 positive cells were ubiquitous ~~within all regions of~~in the IPF lung. In regions of less dense fibrosis, the proliferating cell morphology was macrophages. Mature fibrotic regions and fibroblast foci contained more densely packed structural cells and extracellular matrix where the ki67 positive cells were ~~-~~likely to be myofibroblasts. Within the fibrotic regions, t~~and t~~here was no ~~simple~~ association between the cross-linking and proliferation at the point examined (supplementary figure ~~8~~9).

Transglutaminase inhibition enhances matrix proteolysis

We next asked if abnormal matrix cross-linking conferred resistance to proteolysis. ECM preparations were generated incorporating tritiated proline and the release of tritium into supernatants taken as a measure of matrix proteolysis. In all ECM preparations a low level of spontaneous ECM turnover was observed. Treatment of IPF fibroblasts during ECM deposition with the TG2 inhibitor cystamine increased spontaneous ECM turnover (vehicle 202 DPM vs. cystamine 549 DPM, $P<0.01$, n=3). To determine if the observed spontaneous ECM turnover was due to ECM resident proteases we treated the formed ECM preparations with a broad spectrum protease inhibitor which tended to reduce spontaneous ECM turnover. Addition of active MMP-1 had no further effect on ECM turnover in either control or cystamine treated IPF ECM preparations (figure 6). Direct activation of resident MMPs by the addition of APMA enhanced the turnover of IPF ECM formed in the presence of cystamine from all IPF derived cells however the effect varied between cells and did not achieve significance. Addition of activated MMP-1, -2 or -7 had no additional effect over the APMA vehicle. Cystamine had no effect on control ECM turnover and the LOX family inhibitor βAPN had no effect on proteolysis of either control or IPF derived ECM (supplementary figure 10~~9~~).

***In vivo* inhibition of TG2**

To determine if inhibition of transglutaminases *in vivo* would result in increased ECM turnover and a net reduction in fibrosis we examined the effect of cystamine in the mouse bleomycin model of fibrosis. In preliminary experiments we confirmed that bleomycin treatment of lung tissue resulted in increased transglutaminase activity. *Ex vivo* incubation of murine lung tissue with bleomycin resulted in a 2.2 fold increase in transglutaminase activity ($P<0.001$, n=3) which was almost completely abrogated by cystamine ($P<0.05$, n=3. Figure 7A). Following this we performed a time course and determined that the level of fibrosis no longer increased 24 days after bleomycin administration (supplementary figure 11~~0~~). In the mouse model, cystamine administration from 24 to 34 days post bleomycin exposure was

associated with a 24% reduction in total lung hydroxyproline (vehicle 1593µg vs. cystamine = 1198µg, *P*<0.05, n=3) but had no effect hydroxyproline in saline treated animals (figure 7b).

Discussion

Here we have shown that IPF derived ECM is strongly crosslinked and supports increased fibroblast adhesion and proliferation. Moreover, disruption of ECM cross-linking *in vitro* affects ECM structure and reduces enhanced fibroblast adhesion and proliferation, and inhibition of transglutaminases *in vivo* enhances ECM turnover. Further, expression of TG2 and the LOXL family in IPF are both ECM and cell dependent. Collectively, these findings suggest that IPF ECM is abnormally cross-linked and this cross-linking is one factor which supports fibrosis by enhanced fibroblast growth and resistance to normal ECM turnover.

The induction of the ECM cross-linking enzymes TG2 and LOXL3 by IPF ECM is consistent with the observations of Parker and colleagues who demonstrated that fibrotic ECM induces multiple pro-fibrotic gene expression programs[23]. Collectively, these observations are consistent with fibrotic changes creating an environment that sustains further fibrosis and tissue remodelling. A number of potential mechanisms could explain the enhanced fibroblast adhesion and proliferation on fibrotic ECM. The increased activity of TG2 in IPF derived fibroblasts results in an increase in n-ε-γ-glutamyl lysine cross links between collagen and fibronectin. The alterations in ECM structure as a consequence of increased cross-linking may result in increased access to ECM pro-adhesive and proliferative signals and reduced adhesion and proliferation caused by inhibition of both TG2 and the LOXL family would be consistent with this. The ~~relative~~ larger increase in ~~meatabolic~~metabolic activity (MTT reduction) compared with the more modest increase in DNA synthesis may also suggest that IPF matrix also has effects upon fibroblast metabolism. In addition, transglutaminase activity enhances fibronectin deposition and changes in ECM proteins may affect adhesion and proliferation[12]. Enhanced cross linking may also alter ECM stiffness which is a driver of cell growth, survival and gene transcription however any such effect seems independent of TG2 activity which was unaffected by ECM stiffness in

our study. It is also possible that the cross links themselves are capable of outside-in signaling to fibroblasts enhancing adhesion and proliferation.

Whilst IPF derived cells have higher transglutaminase activity on control ECM, IPF derived ECM induces transglutaminase activity in control fibroblasts. Our data therefore suggest that both the cell and ECM origin determine transglutaminase activity. It is possible the effect of IPF ECM may lead to permanent changes in gene expression. The study by Parker and colleagues suggested that although the ECM was the primary driver of fibrotic gene expression by modulation of the pro-fibrotic micro-RNA miR-29, the cell type contributed synergistically to fibrotic gene expression[24]. Recent genetic studies suggest that IPF fibroblasts may have both genetic[25] and potentially acquired epigenetic differences[26] which may account for differences in gene expression.

The TG2 generated n-ε-γ-glutamyl lysine cross link is resistant to proteolysis by MMP-1 and -2 *in vitro* and reduced cross-linking is likely to explain the increase in ECM turnover induced by the TG2 inhibitor[27]. Interestingly, we observed that ~~that~~ the TG2 inhibitor cystamine enhanced constitutive or spontaneous ECM turnover which was inhibited by a broad spectrum protease inhibitor and enhanced by APMA, an activator of MMPs. ECM proteolysis was not further enhanced by endogenous MMP-1, -2 or -7; proteases overexpressed in the lungs of those with IPF. Our findings are consistent with the presence of MMPs in the ECM preparation causing constitutive ECM turnover. Proteomic analysis of the ECM confirms the presence of multiple collagenolytic MMPs which could be activated by APMA and also ADAMS, serine proteases and cathepsins[28].

In vivo, intra-tracheal administration of bleomycin results in a strong inflammatory reaction leading to collagen deposition resolving over 14 to 21 days followed by the persistence of excess collagen in the absence of inflammation[29]. TG2 is a multi-functional protein with intra and extra-cellular, enzymatic and non-enzymatic actions in inflammation, cell death and survival[30]. In TG2 knockout animals, ~~Bleomycin~~

bleomycin induced lung fibrosis is reduced during the inflammatory and fibrotic phases of the ~~bleomycin~~ We have used a TG2 inhibitor during the established fibrotic phase of the model and observed a small reduction in total lung collagen at a point where the fibrosis had become established. We suspect that in addition to the anti-inflammatory effect on the generation of fibrosis observed by Olsen and colleagues, the effect on lung collagen seen in this model was likely to have been by the reduction in fibrosis driven transglutaminase cross linking allowing protease mediated ECM turnover. The combination of interruption of the proposed TGF-β/TG2 pro-fibrotic feedback loop, reduction of fibroblast growth and restoration of normal ECM turnover may all contribute to reduce the progression of fibrosis[~~11~~12]. Taken together our data suggest that inhibition of TG2 in fibrosis may reduce the burden fibrosis by multiple mechanisms. Recently, inhibition of the cross linking enzyme LOXL2 using a monoclonal antibody proved unsuccessful as a therapy for IPF[31]. The multiple cross-linking enzymes present in fibrotic lung tissue are likely to fulfil different functions and inhibition of TG2 remains a potential target in human lung fibrosis.

In conclusion, we have found that inhibition of TG2 mediated cross-link formation reduces fibroblast adhesion, proliferation and enhances the turnover of ECM produced by IPF fibroblasts. These findings suggest that inhibition of transglutaminase cross-linking may be a potential therapy for IPF.

Figure legends

Figure 1. Expression of cross-linking enzyme transcripts in control and IPF derived fibroblasts. Quantitative gene expression of cross linking enzymes in three control and three IPF derived fibroblasts determined by real time PCR. Lysyl oxidase (*LOX*) was expressed at a very low level. Lysyl Oxidase like protein transcripts (*LOXL*) 1-4 were robustly expressed in control and IPF derived fibroblasts with LOXL3 showing a non-significant trend toward increased expression. Transglutaminase 2 mRNA (*TG2*) was expressed at a significantly higher level in the IPF derived fibroblasts. *TG6* and *TG7* were not detected. α-smooth muscle actin (*ACTA2*) is used as positive control. ***$P<0.001$ Data analysed with multiple unpaired t-test's corrected for multiple comparisons using the Holm-Sidak method. Data presented ±SD, n=3.

Figure 2. ECM cross-linking enzymes and transglutaminase mediated cross-links are expressed in IPF tissue. Immunohistochemical staining showing representative images of control lung and three areas of IPF lung tissue, densely fibrotic, less fibrotic and a fibroblast focus. Sequential sections are stained with haematoxylin and eosin (H+E), picrosirius red to identify collagens, and antibodies against α-smooth muscle actin (αSMA), transglutaminase 2 (TG2), the TG2 generated n-ε γ-glutamyl lysine cross-link and the proliferation marker ki67 (proliferating cells denoted by arrows). –Blue indicates haematoxylin counterstaining of nuclei. Isotype control sections are provided for immuno-stains of IPF tissue. Magnification x420.

Figure 3. IPF derived ECM induces LOXL3 protein and transglutaminase activity. (a) Three control and three IPF derived fibroblasts were cultured on three control and three IPF derived ECM preparations and gene expression for cross linking enzymes quantified by real time PCR. Transglutaminase 2 (TG2) mRNA ~~was~~ tended to be more strongly expressed in IPF fibroblasts irrespective of matrix substrate although this was not significant. LOXL3 was strongly induced on IPF derived ECM in both cell types.

Commented [SJ3]: Is this true?

LOX was weakly expressed on control ECM and further supressed on IPF derived ECM. (b) TG2 cross-linking activity measured in three control and IPF fibroblasts is higher in IPF than control cells. IPF derived matrix enhances TG2 in control but not IPF derived fibroblasts. *P <0.05 (c) LOXL3 protein is strongly induced on IPF derived ECM. ***P <0.0001 (two way repeated measures ANOVA).

Figure 4. IPF derived ECM enhances fibroblast ~~adhesion and~~ adhesion, ~~cellular metabolism~~MTT reduction and DNA synthesis~~growth~~. Adhesion of three control and three IPF derived fibroblasts was quantified on tissue culture plastic (none) and three control and IPF derived ECM preparations and repeated three times. Both matrices significantly enhanced adhesion of normal fibroblasts. IPF matrix significantly enhanced adhesion of both fibroblast types over control matrix. (b) IPF ECM ~~enhances~~increased ~~proliferation metabolic activity~~MTT reduction and DNA synthesis ~~of~~ in cells ~~in the presence of~~treated with 1% foetal bovine serum (FBS) and platelet derived growth factor-bb (PDGF-bb) for 48 hours ~~as assessed by MTT reduction~~(~~,~~ **P<0.05, **P<0.01 and~~,~~ ***P<0.0001~~), (multiple t-tests with Holm-Sidak correction) (two-way repeated measures ANOVA)and also enhanced DNA synthesis as assessed by EdU incorporation under the same conditions (P<0.01 & P<0.05 respectively).~~

Figure 5. Inhibition of cross linking reduces fibroblast adhesion and growth. (a) Scanning electron micrograph of control and IPF fibroblasts growing in their own extra cellular matrix (ECM). Vehicle treated preparations show cross linking ECM strands and webs. Inhibition of transglutaminases with cystamine or the LOX family with β-amino-proprionitrile (βAPN) results in highly disordered ECM with loss of the fibrillary structures. (b) Inhibition of transglutaminases or the LOX family during ECM deposition significantly inhibits fibroblast adhesion on IPF derived but not control ECM (n=3) (c) Inhibition of transglutaminases or the LOX family during ECM deposition significantly inhibits fibroblast growth over 48 hours as assessed by MTT assay. (d) *In vitro* collagen / fibronectin cross-linking by recombinant TG2 significantly enhances control fibroblast adhesion over non cross-linked, vehicle treated collagen / fibronectin. The enhanced adhesion is inhibited by cystamine (cys) (n=3). (e)

In vitro collagen / fibronectin TG2 cross-linking ~~enhances~~ increases control ~~cell~~ fibroblast number the presence of 1% FBS compared with vehicle treated collagen / fibronectin (n=3). * $P<0.05$, ** $P<0.01$.

Figure 6. Tritiated hydroxyproline release from IPF ECM is due to endogenous proteases. Liberation of radio-labelled collagen fragments from EMC derived from IPF fibroblasts treated with either cystamine or vehicle, normalised to scintillant only background. Cystamine treatment of IPF ECM enhances spontaneous ECM turnover which is reduced by a broad spectrum protease inhibitor (protease i) but is not further increased by active MMP-1. * $P<0.05$.

Figure 7. Cystamine inhibits transglutaminase activity and reduces fibrosis *in vivo*. (a) Bleomycin (bleo) treatment of *ex vivo* lung tissue significantly increases transglutaminase activity which is inhibited by cystamine (cys, $P<0.05$, n=3). AU=arbitrary unit of relative transglutaminase activity. (b) Treatment of animals with cystamine from days 24 to 34 post bleomycin instillation reduces total lung hydroxyproline. ** $P<0.01$, * $P<0.05$.

References.

1 Navaratnam V, Fleming KM, West J, et al. The rising incidence of idiopathic pulmonary fibrosis in the UK. Thorax 2011; 66:462-467

2 Bjoraker JA, Ryu JH, Edwin MK, et al. Prognostic Significance of Histopathologic Subsets in Idiopathic Pulmonary Fibrosis. Am. J. Respir. Crit. Care Med. 1998; 157:199-203

3 King Jr TE, Pardo A, Selman M. Idiopathic pulmonary fibrosis. The Lancet; 378:1949-1961

4 Pena A-M, Fabre A, Débarre D, et al. Three-dimensional investigation and scoring of extracellular matrix remodeling during lung fibrosis using multiphoton microscopy. Microscopy Research and Technique 2007; 70:162-170

5 Hynes RO, Naba A. Overview of the Matrisome—An Inventory of Extracellular Matrix Constituents and Functions. Cold Spring Harbor Perspectives in Biology 2012; 4

6 Lu P, Weaver VM, Werb Z. The extracellular matrix: A dynamic niche in cancer progression. The Journal of Cell Biology 2012; 196:395-406

7 Bonnans C, Chou J, Werb Z. Remodelling the extracellular matrix in development and disease. Nat Rev Mol Cell Biol 2014; 15:786-801

8 Page-McCaw A, Ewald AJ, Werb Z. Matrix metalloproteinases and the regulation of tissue remodelling. Nat Rev Mol Cell Biol 2007; 8:221-233

9 Cox TR, Erler JT. Remodeling and homeostasis of the extracellular matrix: implications for fibrotic diseases and cancer. Disease Models & Mechanisms 2011; 4:165-178

10 Selman M, Pardo A, Barrera L, et al. Gene Expression Profiles Distinguish Idiopathic Pulmonary Fibrosis from Hypersensitivity Pneumonitis. Am. J. Respir. Crit. Care Med. 2006; 173:188-198

11 Rosas IO, Richards TJ, Konishi K, et al. MMP1 and MMP7 as potential peripheral blood biomarkers in idiopathic pulmonary fibrosis. PLoS Med 2008; 5:e93

12 Olsen KC, Sapinoro RE, Kottmann RM, et al. Transglutaminase 2 and Its Role in Pulmonary Fibrosis. Am. J. Respir. Crit. Care Med. 2011; 184:699-707

13 Barry-Hamilton V, Spangler R, Marshall D, et al. Allosteric inhibition of lysyl oxidase-like-2 impedes the development of a pathologic microenvironment. Nat Med 2010; 16:1009-1017

14 Grenard P, Bresson-Hadni S, El Alaoui Sd, et al. Transglutaminase-mediated cross-linking is involved in the stabilization of extracellular matrix in human liver fibrosis. Journal of Hepatology 2001; 35:367-375

15 Gao Y, Xiao Q, Ma H, et al. LKB1 inhibits lung cancer progression through lysyl oxidase and extracellular matrix remodeling. Proceedings of the National Academy of Sciences 2010; 107:18892-18897

16 Vadasz Z, Kessler O, Akiri G, et al. Abnormal deposition of collagen around hepatocytes in Wilson's disease is associated with hepatocyte specific expression of lysyl oxidase and lysyl oxidase like protein-2. Journal of Hepatology 2005; 43:499-507

17 Hubbard R, Lewis S, Richards K, et al. Occupational exposure to metal or wood dust and aetiology of cryptogenic fibrosing alveolitis. Lancet 1996; 347:284-289

18 Lu H, Hoshiba T, Kawazoe N, et al. Comparison of decellularization techniques for preparation of extracellular matrix scaffolds derived from three-dimensional cell culture. J Biomed Mater Res A 2012; 100:2507-2516

19 Henderson N, Markwick LJ, Elshaw SR, et al. Collagen I and thrombin activate MMP-2 by MMP-14-dependent and -independent pathways: implications for airway smooth muscle migration. Am J Physiol Lung Cell Mol Physiol 2007; 292:L1030-1038

20 Clements D, Dongre A, Krymskaya VP, et al. Wild Type Mesenchymal Cells Contribute to the Lung Pathology of Lymphangioleiomyomatosis. Plos One 2015; 10

21 Tatler AL, Barnes J, Habgood A, et al. Caffeine inhibits TGFbeta activation in epithelial cells, interrupts fibroblast responses to TGFbeta, and reduces established fibrosis in ex vivo precision-cut lung slices. Thorax 2016; 71:565-567

22 Zuo FR, Kaminski N, Eugui E, et al. Gene expression analysis reveals matrilysin as a key regulator of pulmonary fibrosis in mice and humans. Proceedings of the National Academy of Sciences of the United States of America 2002; 99:6292-6297

23 Parker MW, Rossi D, Peterson M, et al. Fibrotic extracellular matrix activates a profibrotic positive feedback loop. J Clin Invest 2014; 124:1622-1635

24 Parker MW, Rossi D, Peterson M, et al. Fibrotic extracellular matrix activates a profibrotic positive feedback loop. The Journal of Clinical Investigation 2014; 124:0-0

25 Noth I, Zhang Y, Ma S-F, et al. Genetic variants associated with idiopathic pulmonary fibrosis susceptibility and mortality: a genome-wide association study. The lancet. Respiratory medicine 2013; 1:309-317

26 Huang SK, Scruggs AM, McEachin RC, et al. Lung Fibroblasts from Patients with Idiopathic Pulmonary Fibrosis Exhibit Genome-Wide Differences in DNA Methylation Compared to Fibroblasts from Nonfibrotic Lung. PLOS ONE 2014; 9:e107055

27 Zhou X, Jamil A, Nash A, et al. Impaired proteolysis of collagen I inhibits proliferation of hepatic stellate cells: implications for regulation of liver fibrosis. J Biol Chem 2006; 281:39757-39765

28 Naba A, Clauser KR, Hoersch S, et al. The matrisome: in silico definition and in vivo characterization by proteomics of normal and tumor extracellular matrices. Mol Cell Proteomics 2012; 11:M111 014647

29 Moeller A, Ask K, Warburton D, et al. The bleomycin animal model: a useful tool to investigate treatment options for idiopathic pulmonary fibrosis? Int J Biochem Cell Biol 2008; 40:362-382
30 Nurminskaya MV, Belkin AM. Cellular functions of tissue transglutaminase. Int Rev Cell Mol Biol 2012; 294:1-97
31 Gilead Sciences I. Gilead Terminates Phase 2 Study of Simtuzumab in Patients With Idiopathic Pulmonary Fibrosis: Gilead Sciences, Inc., 2016; Jan. 5, 2016 Press Release

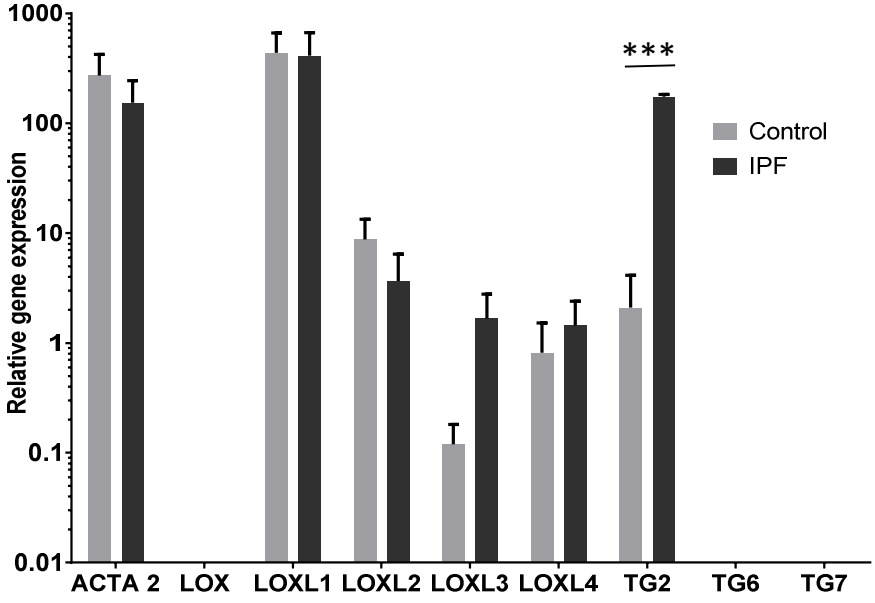
1000
100
10
1
0.1
0.01
Relative gene expression
***
Control
IPF
ACTA 2
LOX
LOXL1
LOXL2
LOXL3
LOXL4
TG2
TG6
TG7

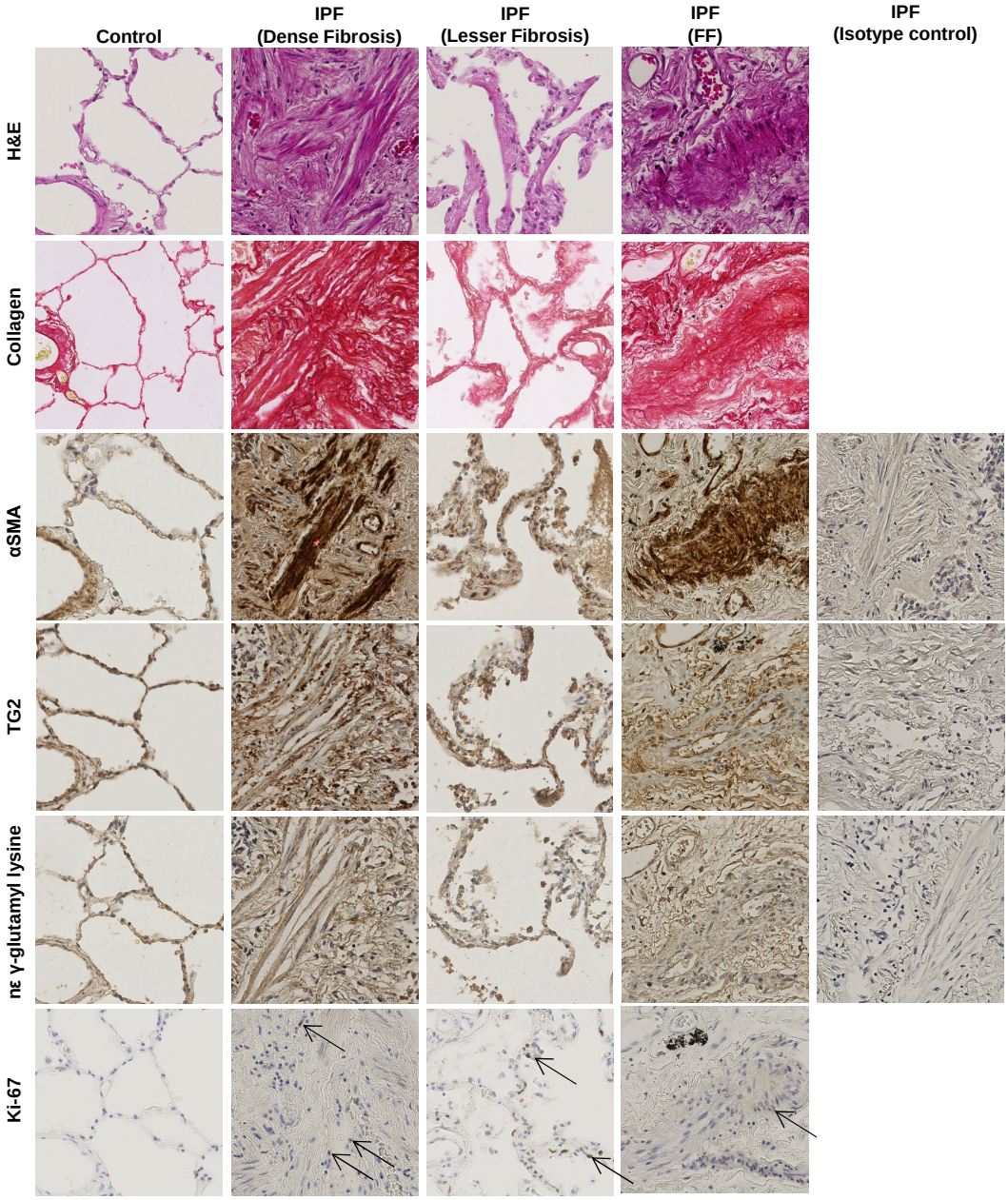
Control
IPF (Dense Fibrosis)
IPF (Lesser Fibrosis)
IPF (FF)
IPF (Isotype control)
H&E
Collagen
αSMA
TG2
nε γ-glutamyl lysine
Ki-67

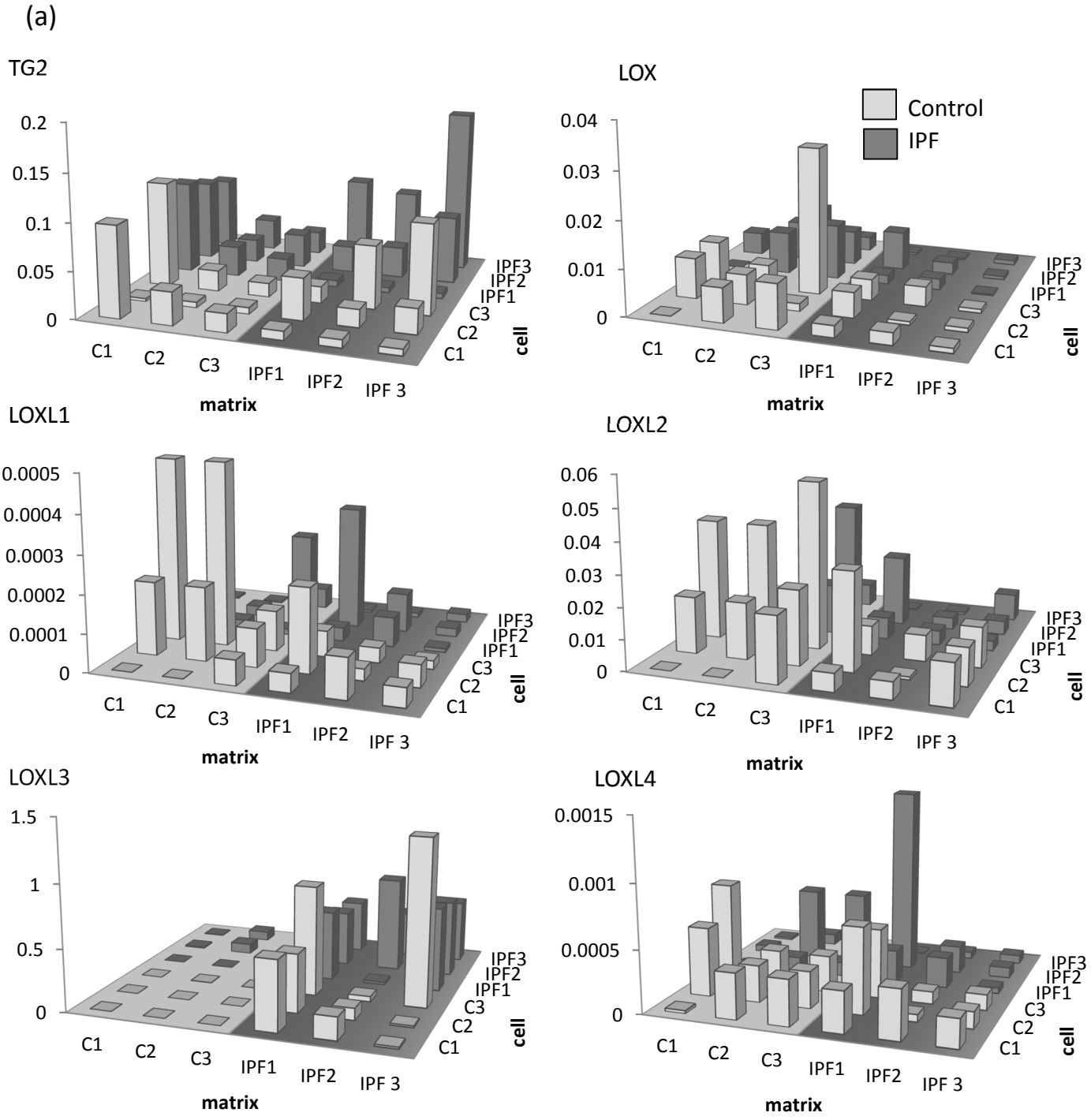
(a)
TG2
LOX
Control
IPF
LOXL1
LOXL2
LOXL3
LOXL4
matrix
cell
C1
C2
C3
IPF1
IPF2
IPF 3
IPF3
(b)
Transglutaminase activity (AU)
Control
IPF
(c)
LOXL3 protein (pg/ml)
control fibroblasts
IPF fibroblasts
***

(a) Adhesion

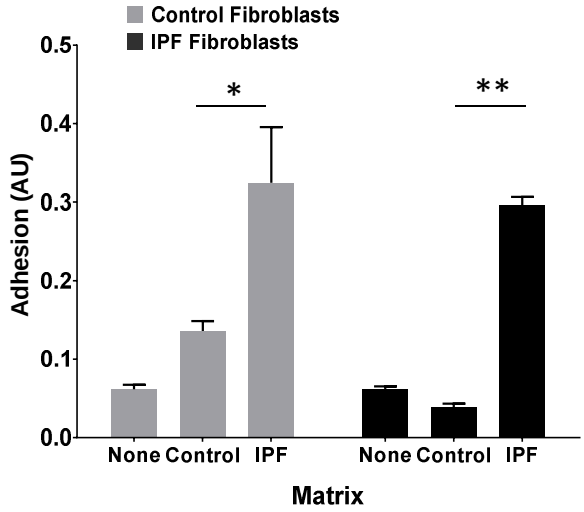

(b) MTT reduction

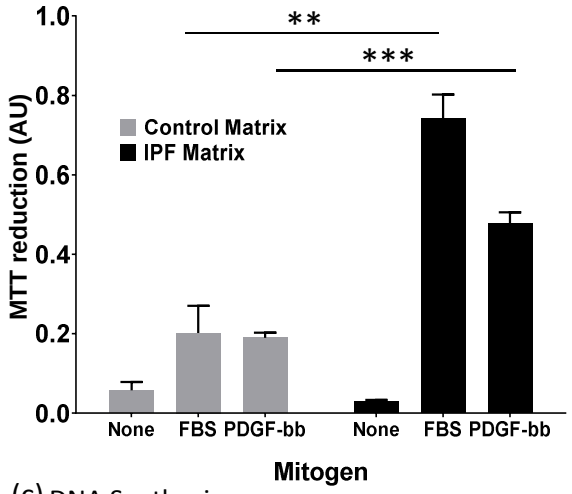

(c) DNA Synthesis

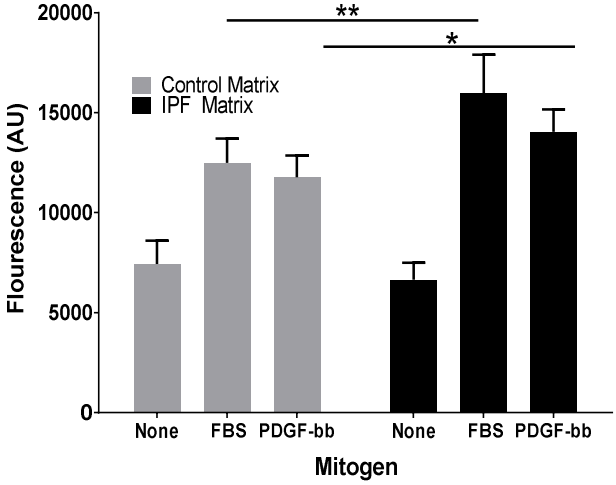

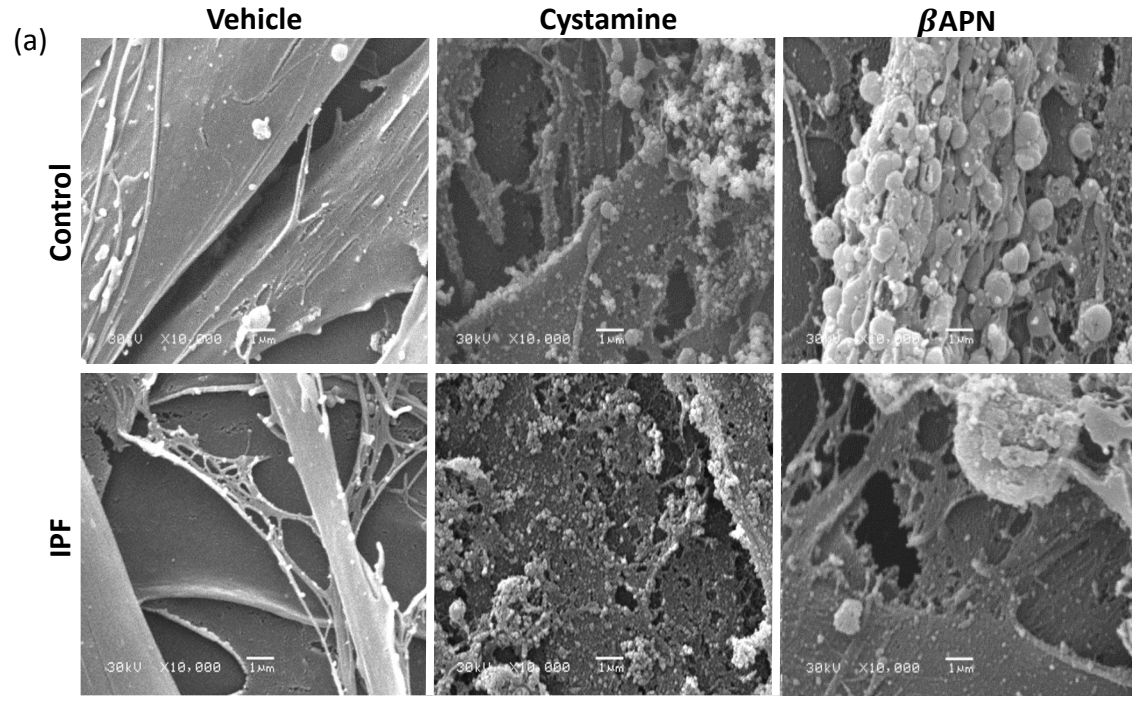
(a)
Vehicle
Cystamine
βAPN
Control
IPF
30kV X10,000 1μm

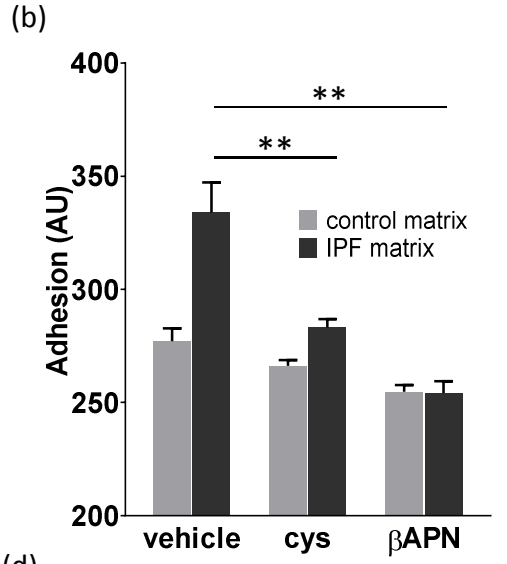
(b)
Adhesion (AU)
400
350
300
250
200
**
**
control matrix
IPF matrix
vehicle
cys
βAPN

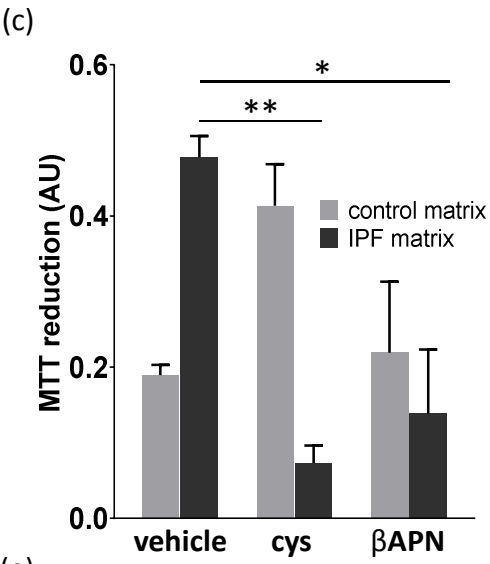
(c)
MTT reduction (AU)
0.6
0.4
0.2
0.0
*
**
control matrix
IPF matrix
vehicle
cys
βAPN

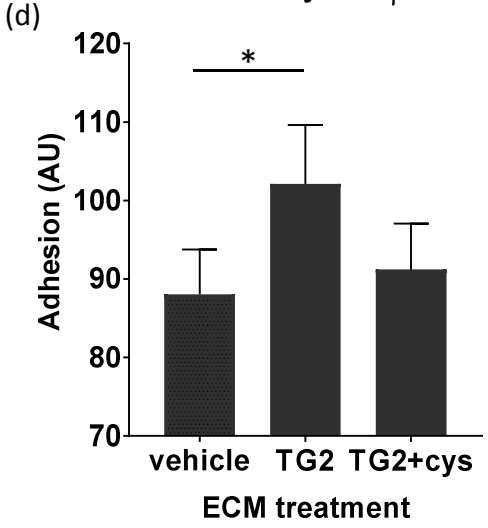
(d)
Adhesion (AU)
120
110
100
90
80
70
*
vehicle
TG2
TG2+cys
ECM treatment

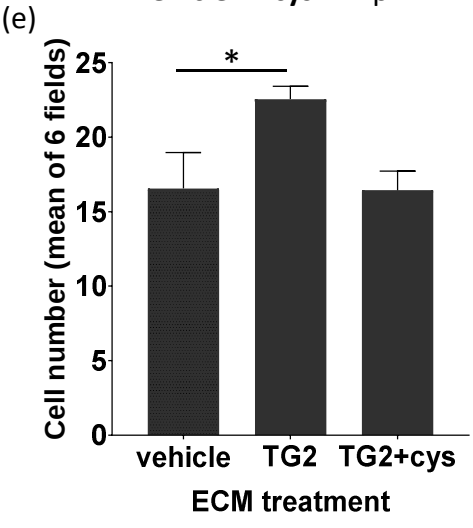
(e)
Cell number (mean of 6 fields)
25
20
15
10
5
0
*
vehicle
TG2
TG2+cys
ECM treatment

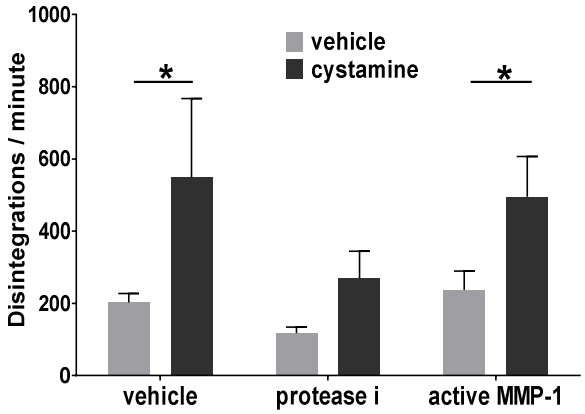
1000
800
600
400
200
0
Disintegrations / minute
vehicle
cystamine
*
*
vehicle
protease i
active MMP-1

(a)

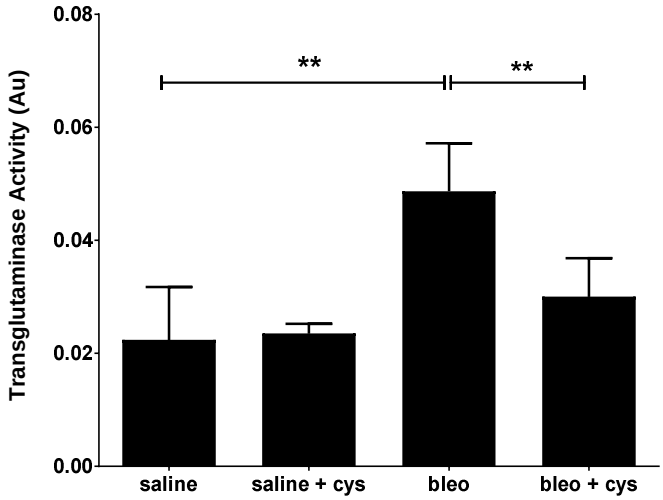
0.08
0.06
0.04
0.02
0.00
Transglutaminase Activity (Au)
**
**
saline
saline + cys
bleo
bleo + cys

(b)

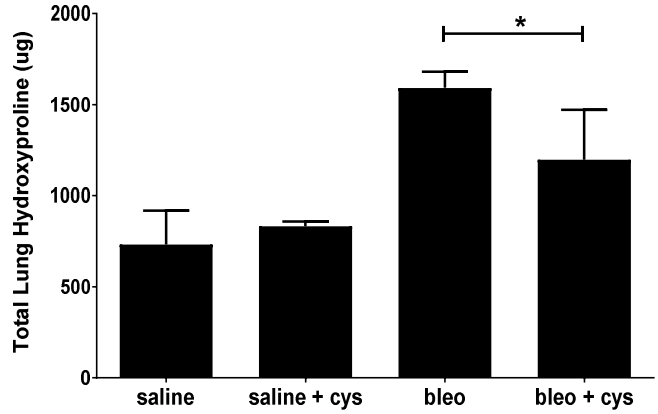
2000
1500
1000
500
0
Total Lung Hydroxyproline (ug)
*
saline
saline + cys
bleo
bleo + cys

Supplementary Figures

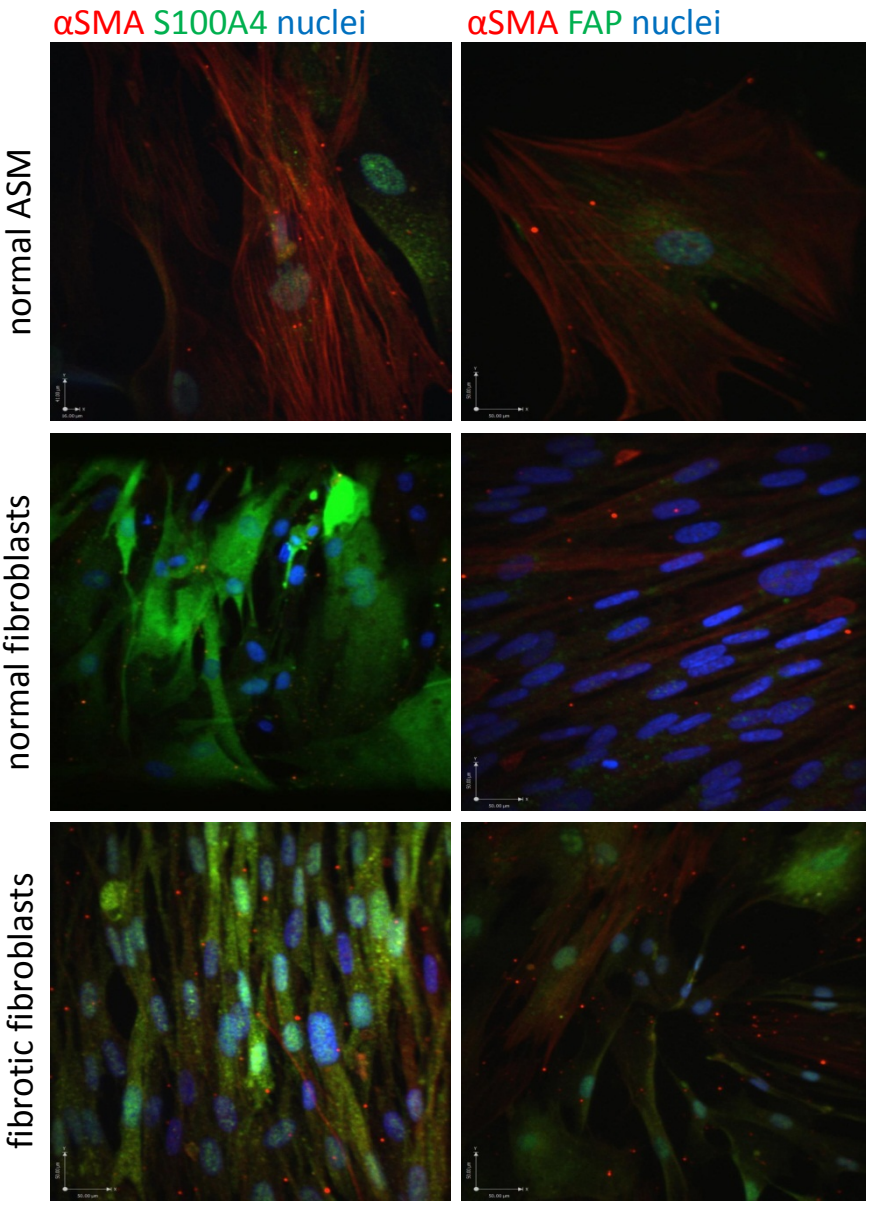
αSMA S100A4 nuclei
αSMA FAP nuclei
normal ASM
normal fibroblasts
fibrotic fibroblasts

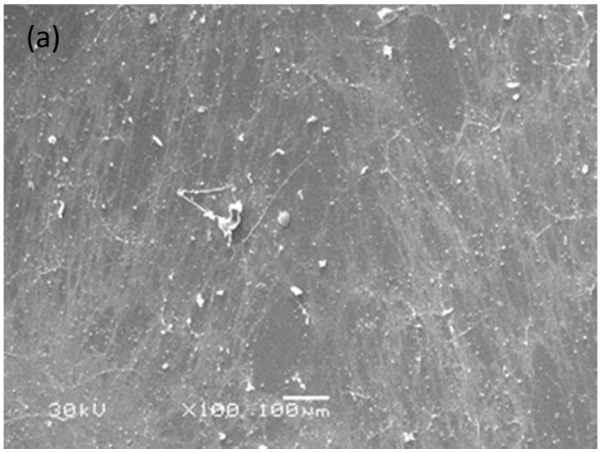
(a)
30kV X100 100µm

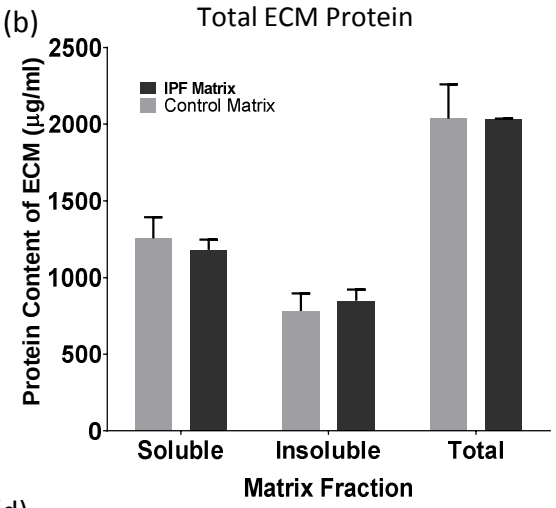
(b)
Total ECM Protein
Protein Content of ECM (µg/ml)
2500
2000
1500
1000
500
0
IPF Matrix
Control Matrix
Soluble
Insoluble
Total
Matrix Fraction

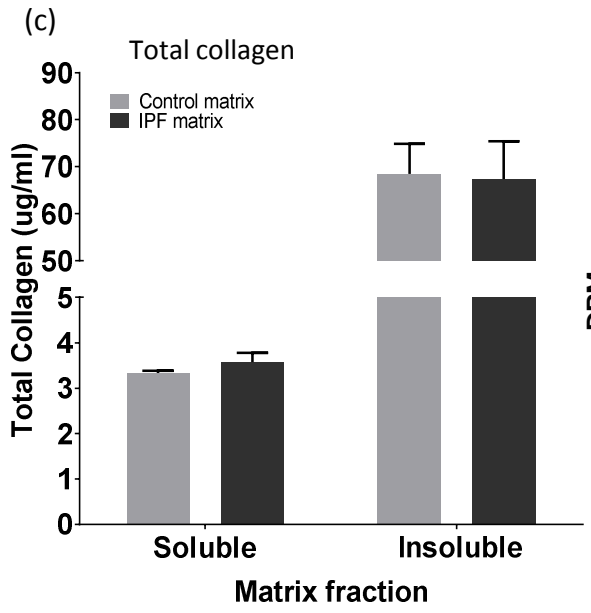
(c)
Total collagen
Total Collagen (ug/ml)
90
80
70
60
50
5
4
3
2
1
0
Control matrix
IPF matrix
Soluble
Insoluble
Matrix fraction

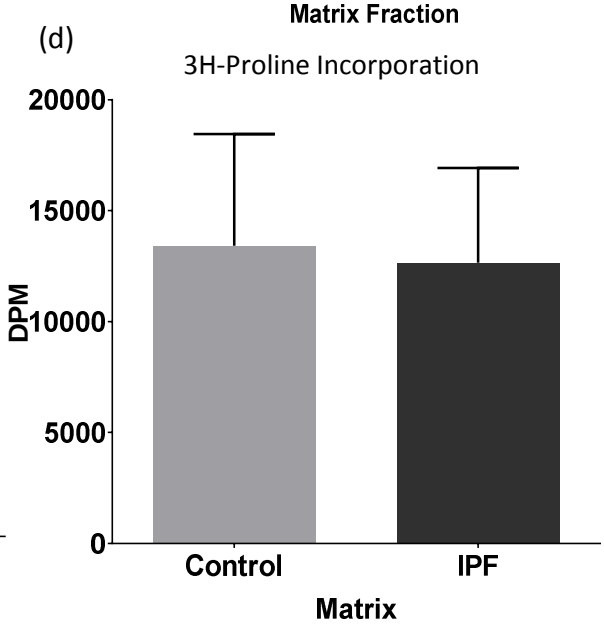
(d)
3H-Proline Incorporation
DPM
20000
15000
10000
5000
0
Control
IPF
Matrix

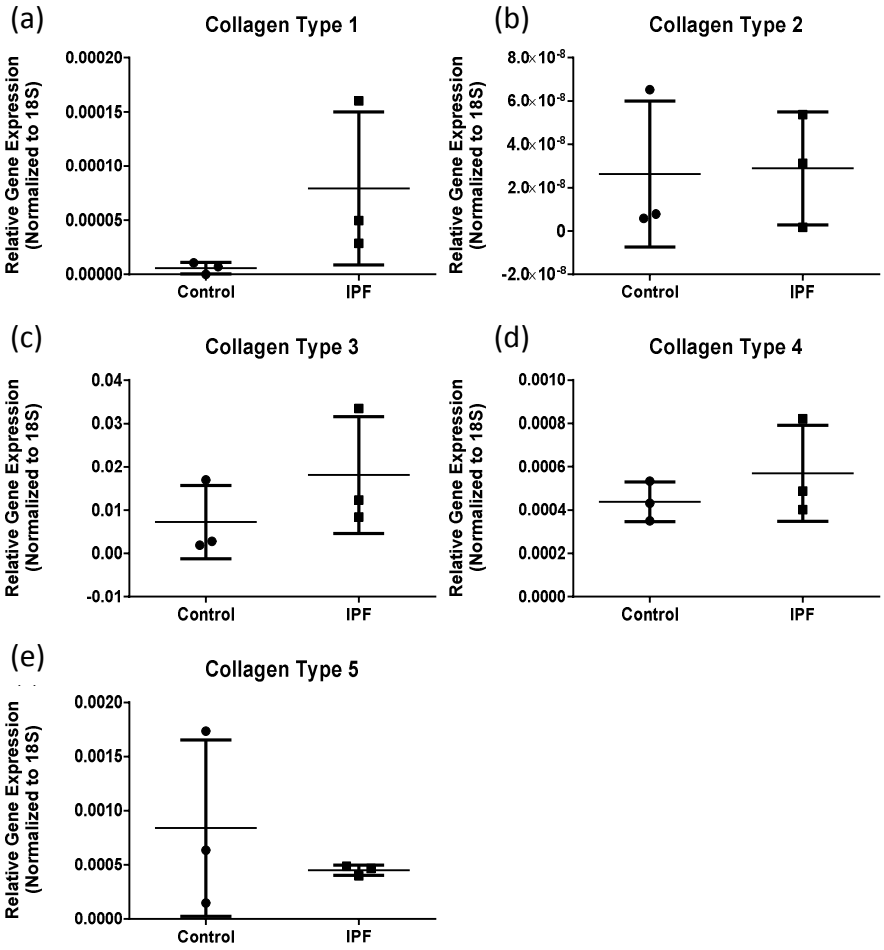
(a)
Collagen Type 1
Relative Gene Expression (Normalized to 18S)
0.00020
0.00015
0.00010
0.00005
0.00000
Control
IPF
(b)
Collagen Type 2
Relative Gene Expression (Normalized to 18S)
8.0×10-8
6.0×10-8
4.0×10-8
2.0×10-8
0
-2.0×10-8
Control
IPF
(c)
Collagen Type 3
Relative Gene Expression (Normalized to 18S)
0.04
0.03
0.02
0.01
0.00
-0.01
Control
IPF
(d)
Collagen Type 4
Relative Gene Expression (Normalized to 18S)
0.0010
0.0008
0.0006
0.0004
0.0002
0.0000
Control
IPF
(e)
Collagen Type 5
Relative Gene Expression (Normalized to 18S)
0.0020
0.0015
0.0010
0.0005
0.0000
Control
IPF

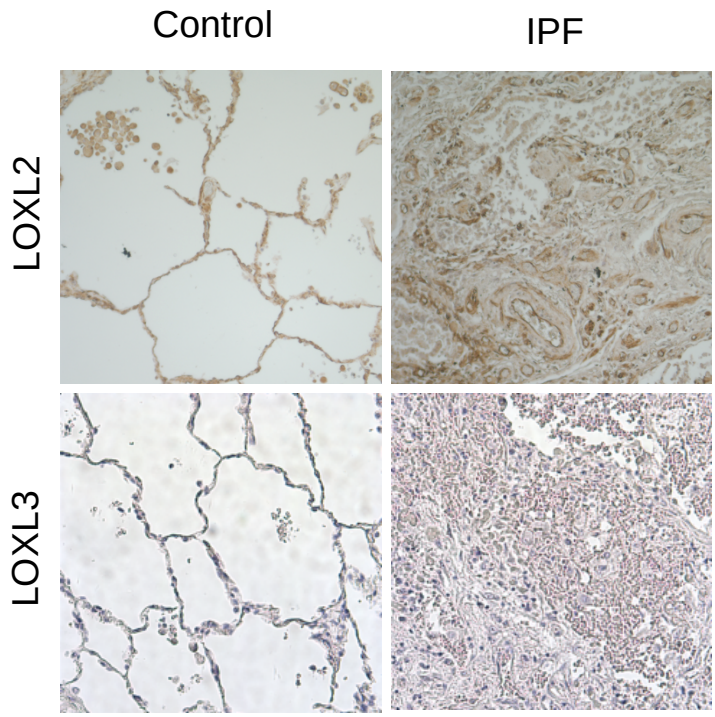
Control
IPF
LOXL2
LOXL3

TG2

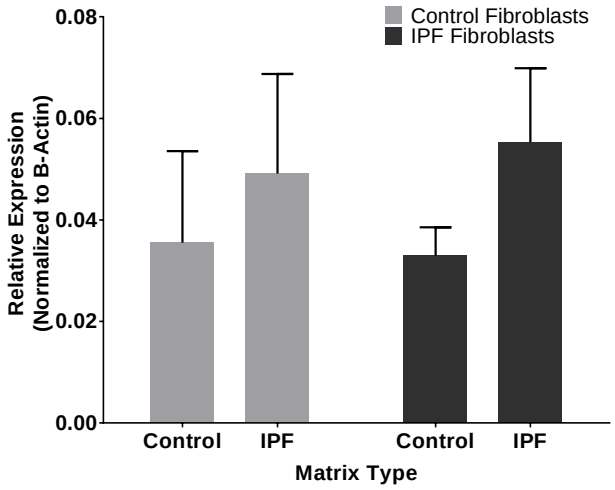

LOX

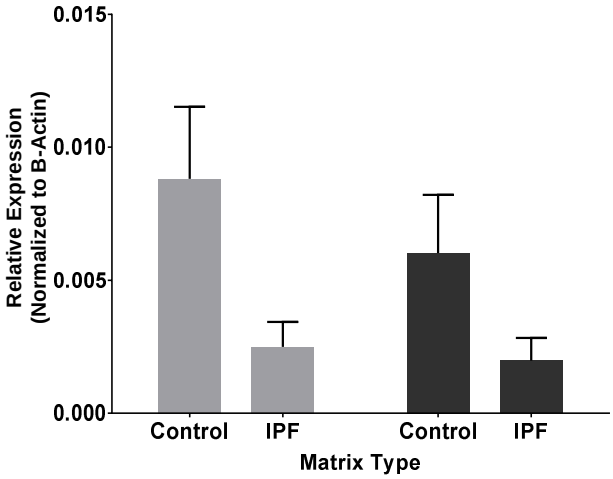

LOXL1

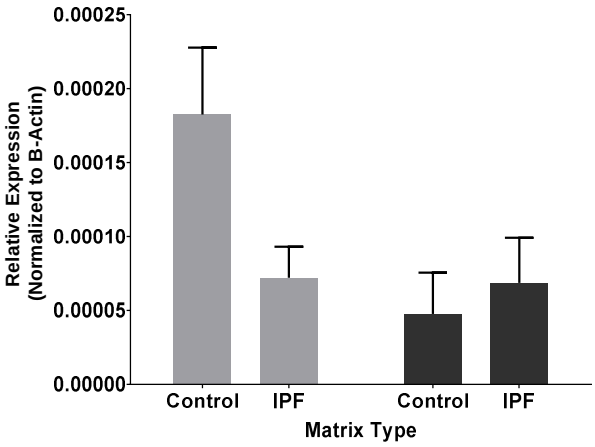

LOXL2

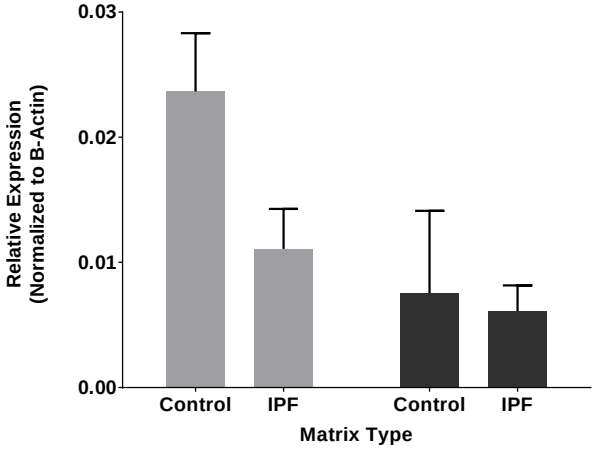

LOXL3

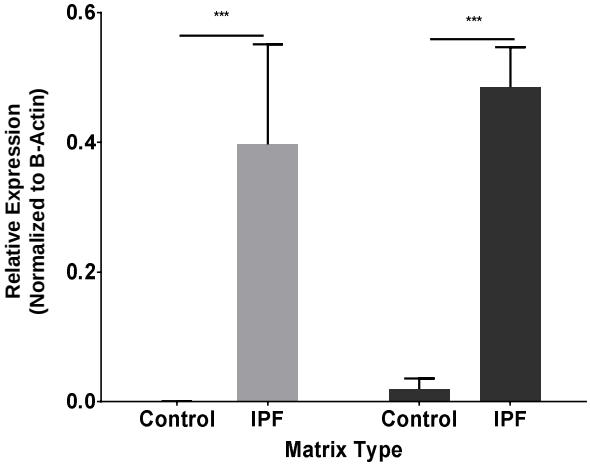

LOXL4

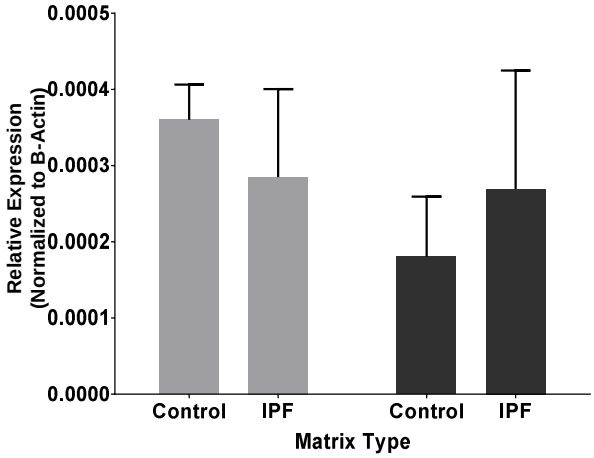

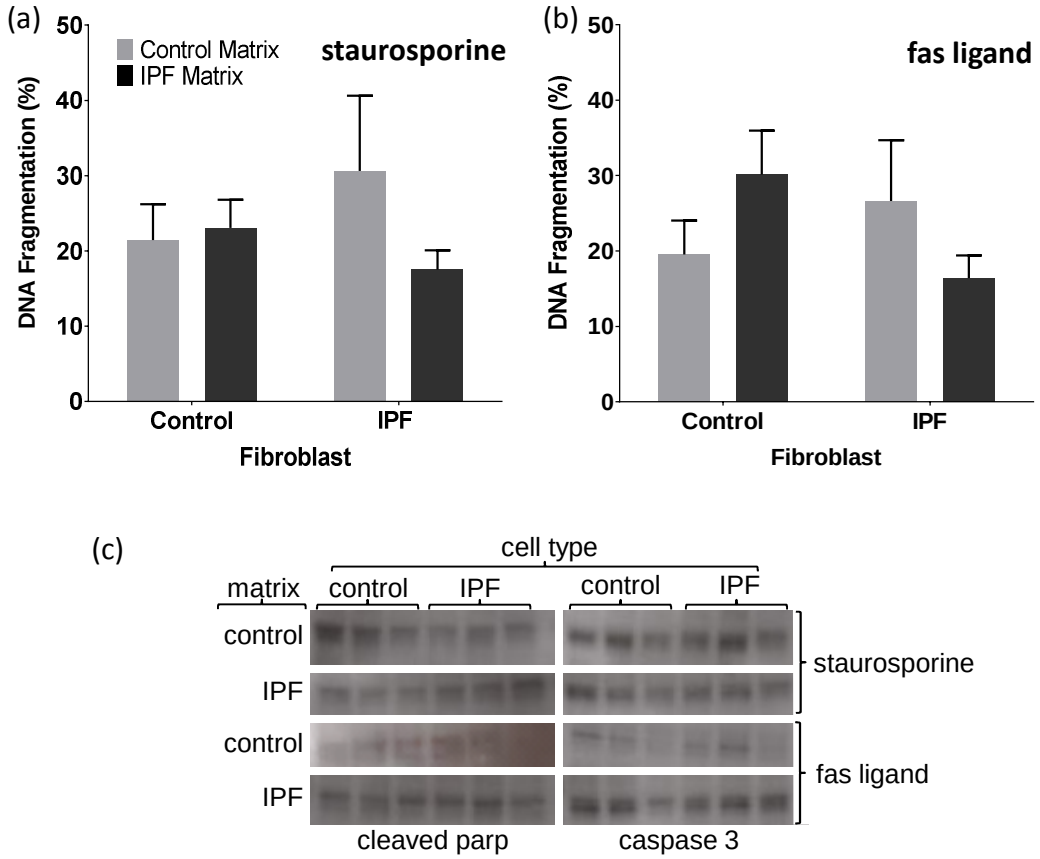
(a)
Control Matrix
IPF Matrix
staurosporine
DNA Fragmentation (%)
50
40
30
20
10
0
Control
IPF
Fibroblast
(b)
fas ligand
DNA Fragmentation (%)
50
40
30
20
10
0
Control
IPF
Fibroblast
(c)
cell type
matrix
control
IPF
control
IPF
control
IPF
control
IPF
staurosporine
fas ligand
cleaved parp
caspase 3

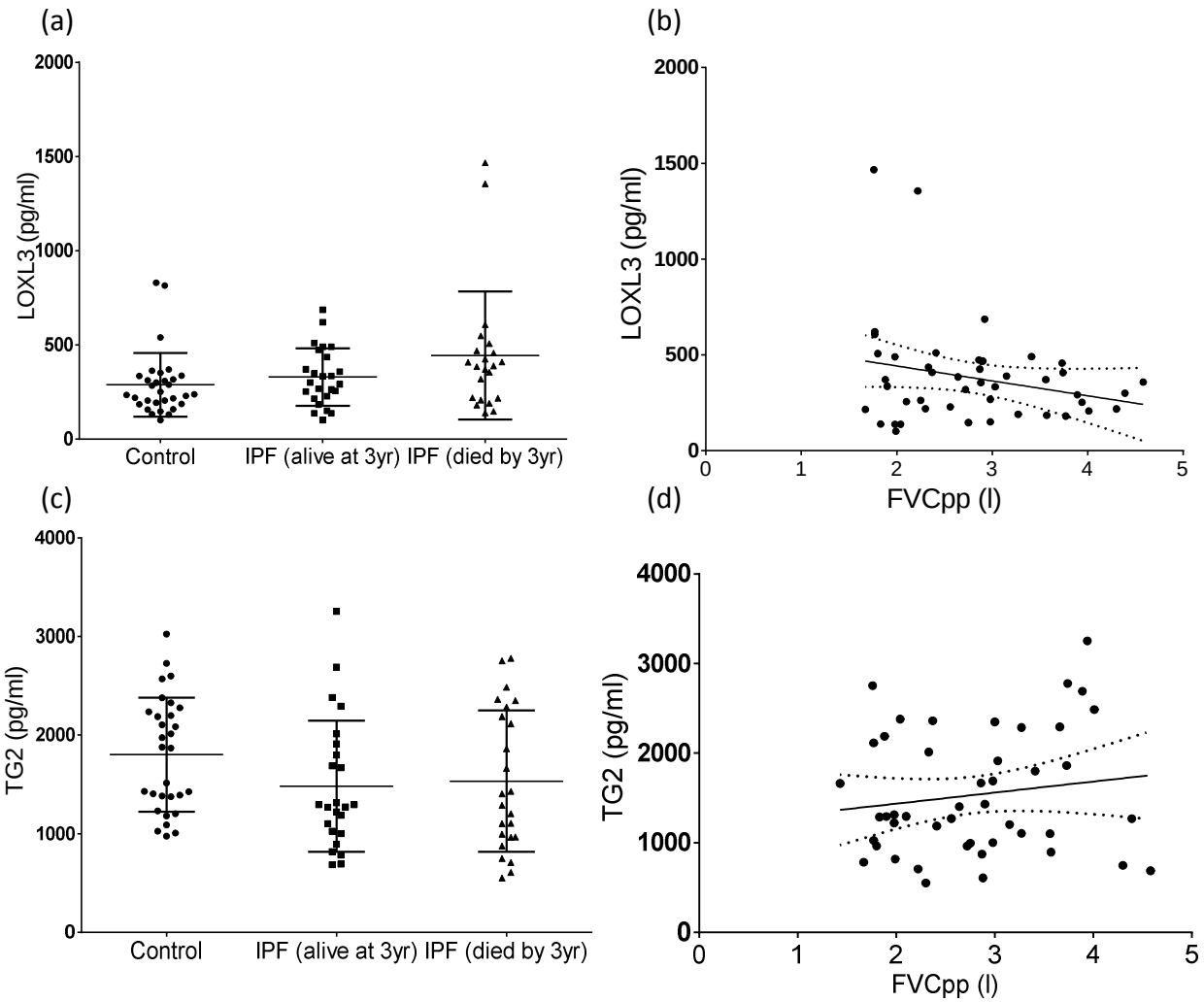
(a)
LOXL3 (pg/ml)
2000
1500
1000
500
0
Control
IPF (alive at 3yr)
IPF (died by 3yr)
(b)
LOXL3 (pg/ml)
2000
1500
1000
500
0
0
1
2
3
4
5
FVCpp (l)
(c)
TG2 (pg/ml)
4000
3000
2000
1000
0
Control
IPF (alive at 3yr)
IPF (died by 3yr)
(d)
TG2 (pg/ml)
4000
3000
2000
1000
0
0
1
2
3
4
5
FVCpp (l)

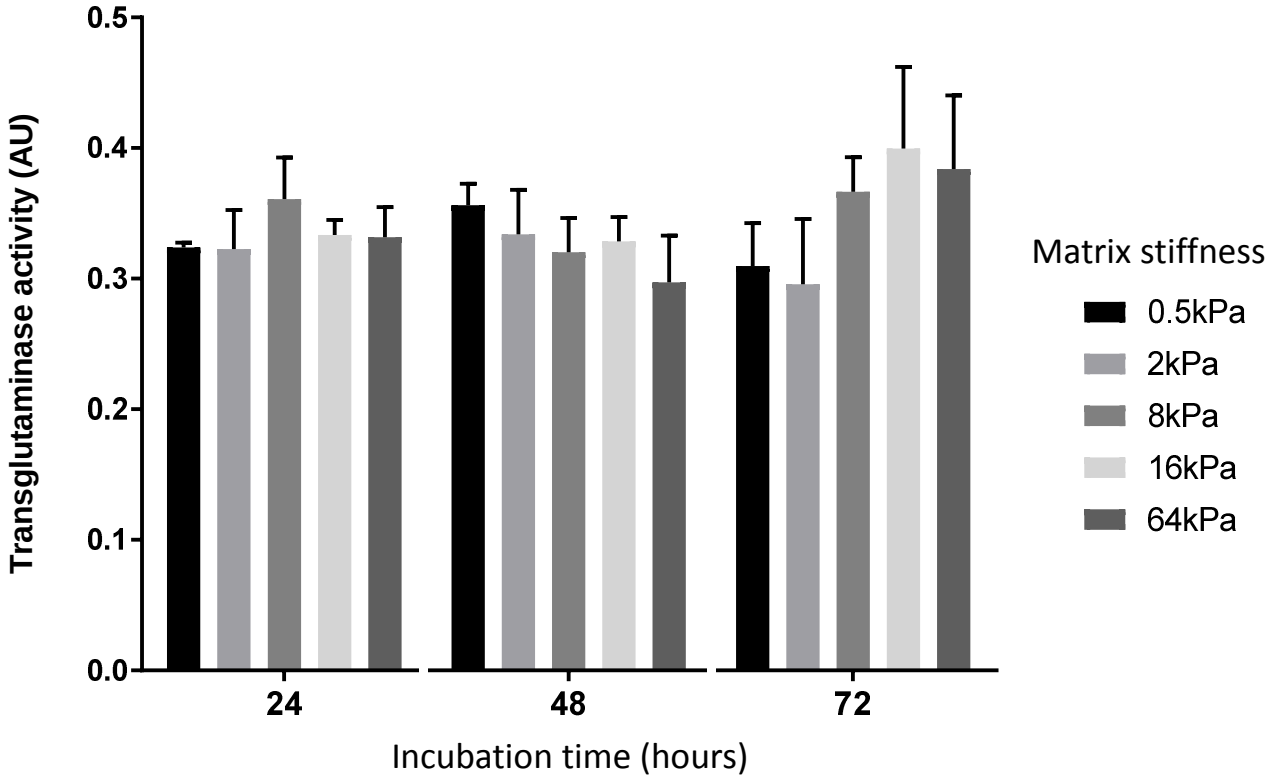
Transglutaminase activity (AU)
0.5
0.4
0.3
0.2
0.1
0.0
24
48
72
Incubation time (hours)
Matrix stiffness
0.5kPa
2kPa
8kPa
16kPa
64kPa

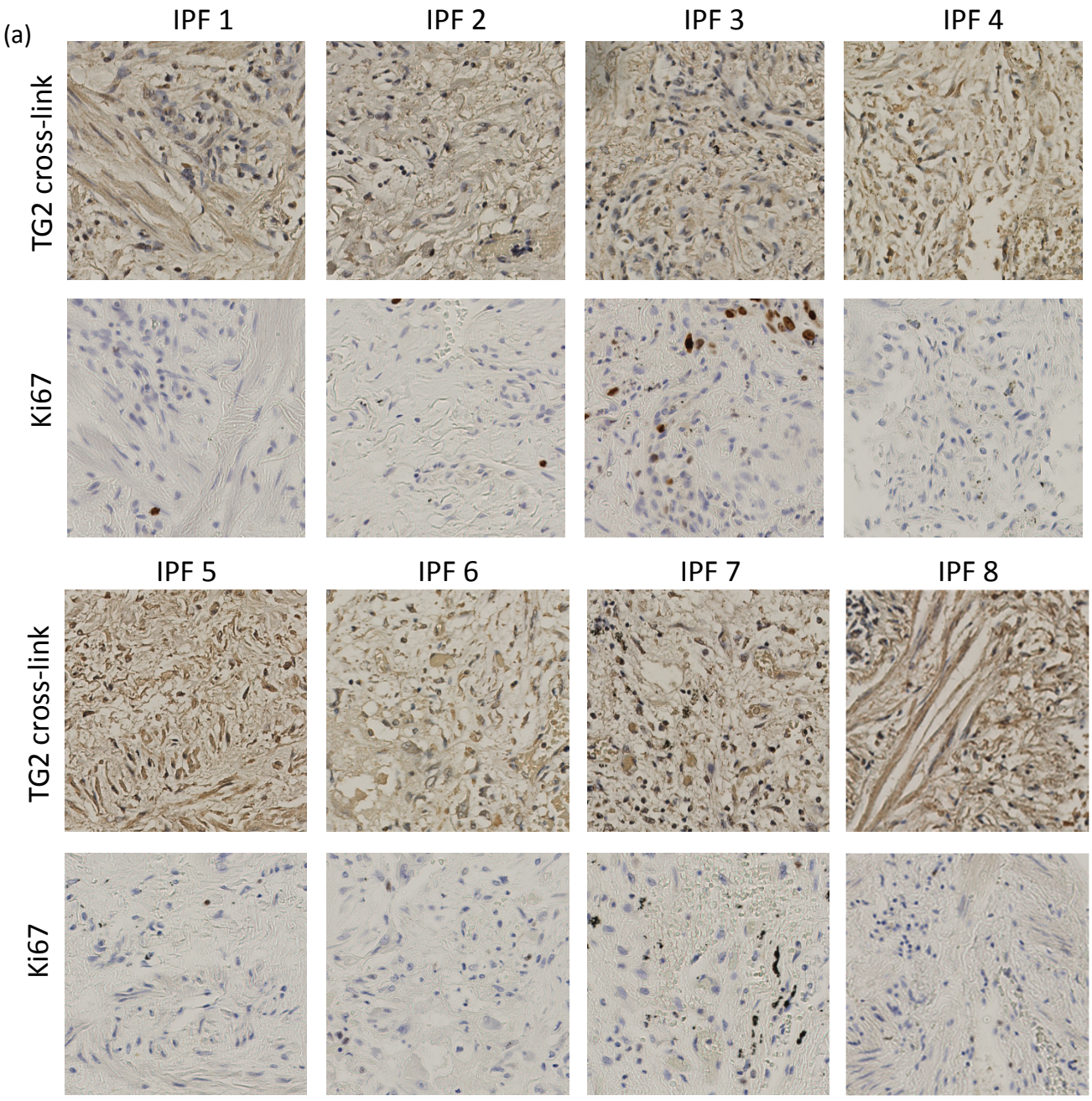
(a)
IPF 1
IPF 2
IPF 3
IPF 4
TG2 cross-link
Ki67
IPF 5
IPF 6
IPF 7
IPF 8
TG2 cross-link
Ki67

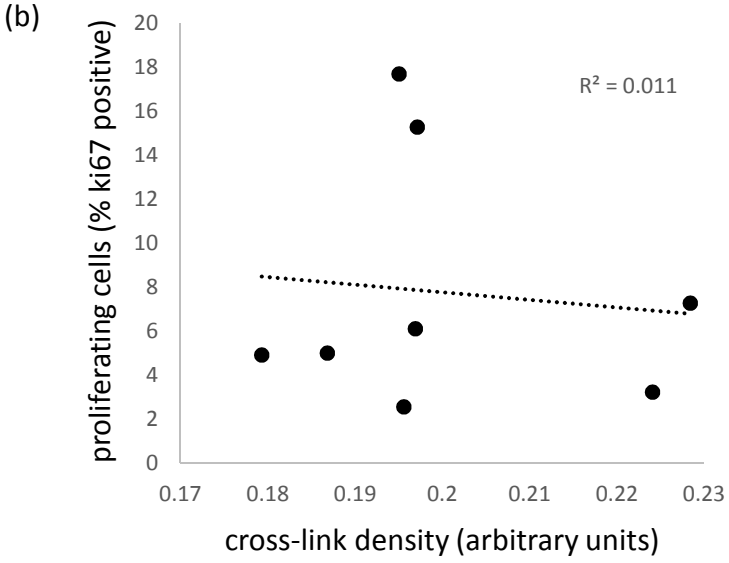
(b)
proliferating cells (% ki67 positive)
20
18
16
14
12
10
8
6
4
2
0
R² = 0.011
0.17
0.18
0.19
0.2
0.21
0.22
0.23
cross-link density (arbitrary units)

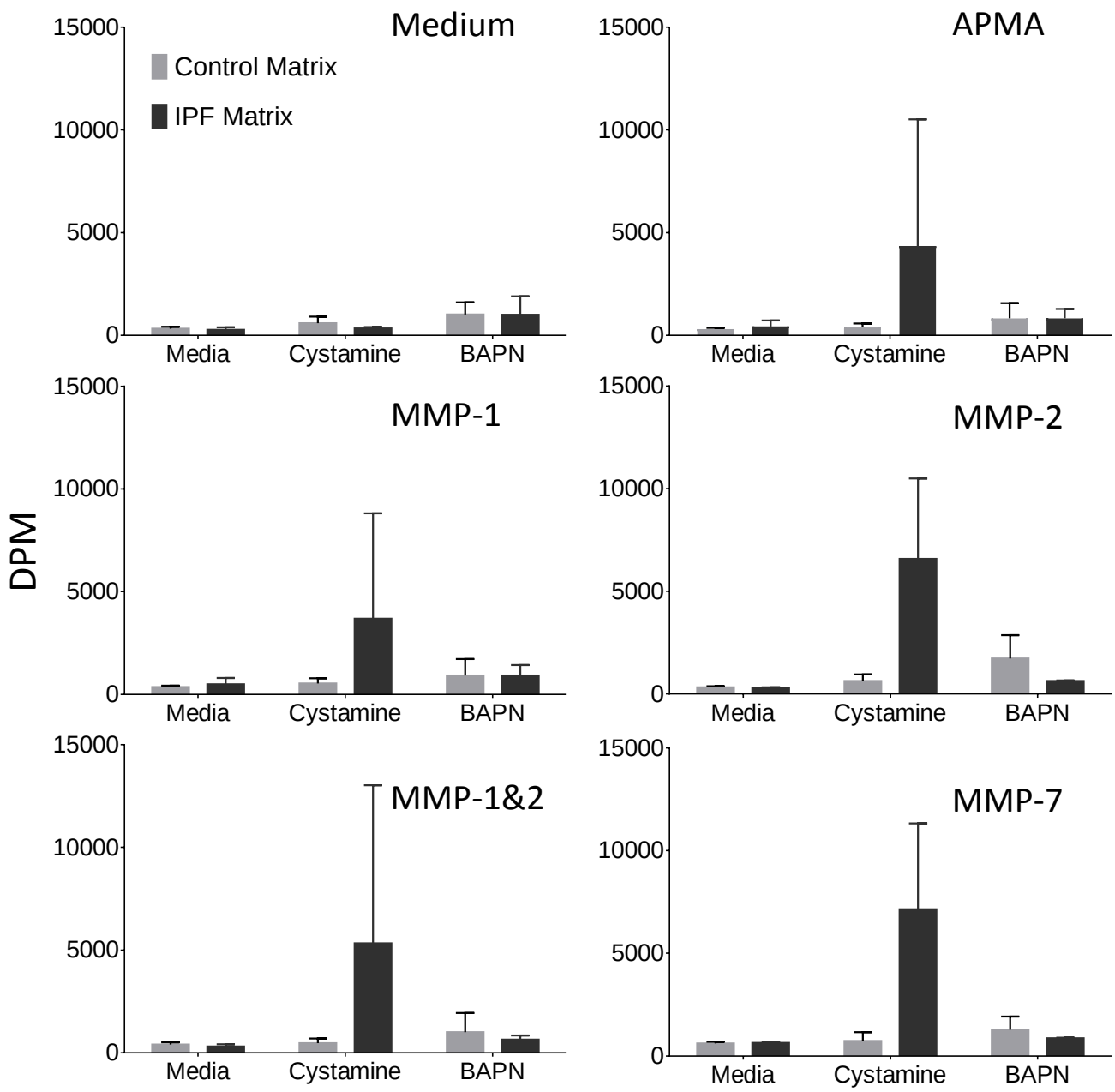
Medium
Control Matrix
IPF Matrix
APMA
MMP-1
MMP-2
MMP-1&2
MMP-7
DPM
15000
10000
5000
0
Media
Cystamine
BAPN

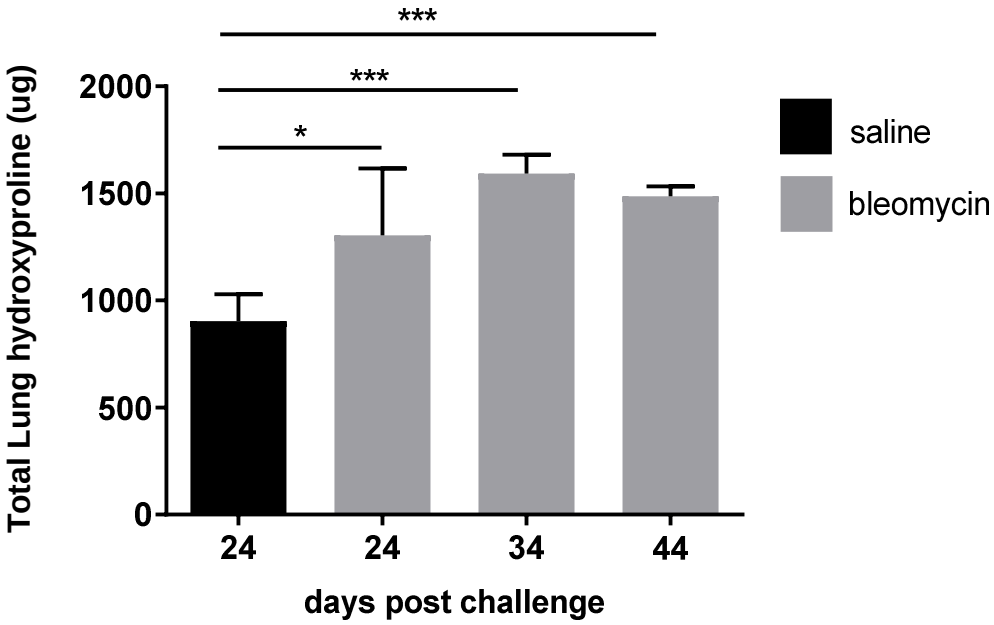
***
***
*
2000
1500
1000
500
0
Total Lung hydroxyproline (ug)
24
24
34
44
days post challenge
saline
bleomycin

Online Data Supplement

ECM crosslinking enhances fibroblast growth and protects against matrix proteolysis in lung fibrosis.

Christopher J Philp[1], Ivonne Siebeke[1], Debbie Clements[1], Suzanne Miller[1], Anthony Habgood[1], Alison John[1], Vidya Navaratnam[2], Richard B Hubbard[2], Gisli Jenkins[1] and Simon R Johnson[1]

[1]*Division of Respiratory Medicine, School of Medicine, University of Nottingham.*

[2]*Division of Epidemiology and Public Health, School of Medicine, University of Nottingham.*

Supplementary Methods

Primary cell isolation and culture

IPF fibroblasts are obtained from surplus lung parenchymal tissue from patients undergoing lung resections for the diagnosis of interstitial lung disease. Control fibroblasts are obtained from otherwise normal tissue distant from lung cancer resections. All patients had a pathological diagnosis of usual interstitial pneumonia and a clinical diagnosis of IPF. Tissue collection is approved through the Nottingham University Hospitals biobank and all patients give written, informed consent. Tissue was dissected into small 3mm cubes and placed in T25 culture flasks. DMEM + 10% FCS, 4mM L-glutamine, 200U/ml penicillin, 200ug/ml streptomycin and 5ug/ml amphotericin B was added and fibroblasts grown out. At passage 2, media was changed and all antibiotic and antimycotic agent concentrations halved. At passage 3, all antibiotic and antimycotic agents were withdrawn, resulting in fibroblasts in DMEM + 10% FCS. Cells are characterised morphologically and by immunostaining for fibroblast specific protein, fibroblast activation protein and smooth muscle actin. Cells are used at passages 2-5. Airway smooth muscle cells extracted from large airways of patients who had died due to non-respiratory causes were used for comparison purposes and have been described previously [1].

Immunofluorescence

Cells were grown in chamber slides, fixed with formaldehyde, permeabilised using 0.15% Triton X-100, blocked with 10% Goat Serum overnight at 4 °C. Antibodies were incubated at 1:250, at room temperature for 1 hour, washed and incubated using a secondary flourophore conjugated antibody, washed then further incubated with CY-3 directly conjugated anti α-SMA (Sigma Aldrich, UK). In the final wash, DAPI (Sigma Aldrich, UK) was added to the PBS at 1:1000. Slides were removed and mounted using Dako Fluorescent Mounting Medium (Dako, Glostrup, Denmark). Slides were imaged using an Improvision spinning disc confocal microscope using Volocity 3D image analysis software (Perkin Elmer, Massachusetts, USA).

Total RNA Extraction

Total RNA was extracted from cultures at approximately 80% confluence in 6 well plates (~$1x10^6$ cells) using the GenElute™ Mammalian Total RNA Miniprep Kit (Sigma Aldrich, Dorset, UK). On-Column DNase I Digestion Set (Sigma Aldrich, Dorset, UK) was used during RNA extraction to remove genomic DNA contamination and prevent false positive PCR traces. RNA was eluted in 30µl of the elute solution and analysed on a NanoDrop (Fisher Scientific, UK) for quantity and quality.

cDNA Synthesis

cDNA was synthesised using Superscript First-Strand Synthesis System (Invitrogen, UK) to the manufacturers specifications.

Real Time PCR

Quantitative RT-PCR was conducted to assess the relative abundance of gene transcripts. SensiFAST SYBR No-ROX Master Mix (Bioline Reagents Ltd., UK) was used as master mix when plating out PCR reactions. Reactions were run using the Mx3005P qPCR System with MxPro Software (Agilent Technologies, CA, USA). Predesigned KiCqStart SYBR Green primers were obtained from Sigma Aldrich (Dorset, UK). PCR data was analysed using the 2-δct method (Livak and Schmittgen, 2001, Rao et al., 2013) which provides normalisation to an endogenous reference in differing cDNA added to the reaction mixture. As total copy number is not a goal of these experiments, relative quantification is suitable as no standard curve is needed. Internal controls were validated to show that there was little variation of housekeeping gene expression with experimental protocols.

Data Analysis, Statistics and Graphical Software

Unless otherwise stated, all data were processed using Microsoft Excel 2010 (Microsoft, USA) and graphed and analysed using Prism V6 (GraphPad Software, USA). Unless otherwise stated, n=3 experimental data are presented with ± standard deviation (SD). Statistics were performed on data using Prism V6 (GraphPad Software, USA).

Immunohistochemistry

Paraffin embedded tissue was deparaffinised using Histoclear (National Diagnostics) and rehydrated in a graded alcohol series. Antigen retrieval was performed using a low pH citrate based antigen unmasking solution in a steamer. Endogenous peroxidases were quenched using 3% hydrogen peroxide and blocked with 2.5% Normal Horse Serum (Vector Laboratories). Antibodies were diluted in blocking agent. Both Impress Anti-Mouse and Impress Anti-Rabbit secondary antibody kits were obtained from Vector laboratories and performed to their manufactures specifications. Colour was developed using DAB Peroxidase (HRP) Substrate Kit (Vector Laboratories) and counterstained with Haematoxylin. Slides were mounted with a glass cover slip and Vectamount permanent mounting medium (Vector Laboratories, CA, USA).

MTT Assay

$1x10^6$ fibroblasts were seeded onto each ECM preparation and incubated with either serum free DMEM, DMEM+1% FCS, DMEM+5ng/ml PDGF-bb or 20ng/ml PDGF-bb for 72 hours then incubated with 0.5mg/ml Thiazolyl Blue Tetrazolium Bromide (Sigma Aldrich) in DMEM/F12 phenol red free media (Life Technologies) for 6 hours, 1ml of isopropanol added to and colour read in triplicates in a 96 well plate and the absorbance read at 595nm, with background subtraction at 690nm, in the Flexstation 3 (Molecular Devices, CA, USA).

Adhesion Assay

Control fibroblasts were incubated with CellTracker Green CMFDA Dye (Life Technologies, UK) at 5µM final concentration in DMEM+10%FBS for 30 minutes. Cells were trypsinised, resuspended in serum free DMEM, seeded onto the ECM preparations and incubated for 2 hours at 37°C. Media and non-

adherent cells were aspirated, the plate washed with PBS and average fluorescence of each sample at Abs. 492 / Em. 517nm using flexstation 3 (Molecular Devices, CA, USA).

Apoptosis assays

Following overnight incubation on 3 IPF and 3 control derived ECM preparations, control fibroblast apoptosis was induced by 1μM Staurosporine or 100ng/ml Fas ligand in serum free DMEM for 24 hours. Samples were then lysed in RIPA buffer for western blot analysis of Caspase 3 activation and PARP cleavage. DNA fragmentation was also determined using the In Situ Cell Death Detection Kit (fluorescin) (Roche Diagnostics Ltd., UK) and counter stained with DAPI for total nuclei counts. Fluorescein-dUTP positive cells were identified by confocal microscopy and expressed as a percentage of the total cells in a fixed field of view using three fields per sample.

DNA Synthesis Assay

To determine the number of proliferating cells through an independent method, a DNA synthesis approach was taken. Cells were cultured in the same way as described above for the MTT assay. To directly measure new DNA synthesis the Click-iT® EdU Microplate Assay was used (Life Technologies) to manufacturers specifications with a final concentration of 10μM EdU and incubation time of 24 hours. The 96 well plate was read with excitation/emission of 568/585nm using the Flexstation 3 (Molecular Devices).

ECM preparation and quantification

Cultures were grown in DMEM+10% FBS to confluence and for a further 3 days to ensure sufficient matrix deposition. Culture media was aspirated and frozen at -20°C for later analysis. Cultures were washed with Phosphate Buffered Saline (PBS). Decellularization was adapted from a previously described method[2]. Cultures were incubated at room temperature with 50mM NH_4OH + 0.05% Triton X-100 (Sigma Aldrich, Dorset, UK) in PBS for 15 minutes or until cells were no longer visible under 10x magnification on a Nikon Diaphot 300 Inverted Microscope (Nikon UK Limited, UK). Ammonium hydroxide and triton solution was aspirated and the cultures briefly washed with 50mM NH_4OH. Following this, all plates were washed 3 times with PBS. Upon completion, all liquid was aspirated and all dishes were incubated at 37°C with 20 U/mL DNase I (Sigma Aldrich, Dorset, UK) to remove DNA contamination for 1 hour then washed 3 times with PBS before further experimentation. This resulted in a cell free and intact ECM as confirmed by SEM.

A two stage extraction process was used as described by Ngoka[3] with the following modifications. RIPA buffer and Complete Mini Protease Inhibitor Cocktail + EDTA was added to ECM preparations and incubated at room temperature for 5 minutes on a platform rocker and aspirated. Urea Lysis Buffer (PBS, pH 7.4, 5.0 M Urea, 2.0 M Thiourea, 50 mM DTT, 0.1% SDS) was then applied for 5 minutes at room temperature on a platform rocker. ECM extracts were dialysed using Slide-A-Lyzer G2 0.5mL/2K MWCO cassettes (Thermo Fisher Scientific Inc., USA) and stored at -20°C.

Total protein assays were performed using a Bio-Rad Total Protein Assay Kit according to the manufactures specifications. To measure total collagen, ECM samples were subjected to acid hydrolysis. Solubilised ECM is diluted 1:1 with 12M HCl, incubated for 20 hours at 95 °C, centrifuged for 10 minutes at 13,000xg and supernatants assayed using the Total Collagen Assay Kit (Quickzyme Biosciences, NL) according to the manufacturer's specification.

Collagen synthesis assay medium was supplemented with tritiated proline to a final activity of 1 μCi/ml (Perkin Elmer, MA, USA), decellularized as described. Solubilised samples were transferred to

scintillation vials containing 10mls of Ultima Gold XR Scintillation fluid (Perkin Elmer) was added to each vial and the radioactivity read on a LKB Wallac 1214 Rackbeta Liquid Scintillation Counter (Perkin Elmer, USA).

Generation of transglutaminase 2 ECM crosslinking in vitro

Cross-linked collagen/fibronectin substrates were generated by incubating 50ug/ml collagen type 1 (Advanced Biomatrix, USA) with 50ug/ml fibronectin (Sigma Aldrich, UK) diluted in serum free DMEM (Sigma Aldrich, UK) in the presence of recombinant TG2 to a final concentration of 500ng/ml. Control collagen/fibronectin mixtures were incubated with either PBS vehicle control, or TG2 (500ng/ml) pre-incubated with the TG2 inhibitor cystamine (0.5mM) for 15 minutes at 37°C. Mixtures were incubated overnight in a shaking incubator at 37°C in six well plates. Prior to seeding, any remaining solution was aspirated, substrates washed in PBS and fibroblasts seeded at 150,000 cells per well in DMEM + 1% FBS. Adhesion and proliferation were assessed as previously described.

ECM Proteolysis Assay

1×10^6 cells/well are plated in 6 well plates and media was supplemented with L-[2,3,4,5-3H]-Proline to a final activity of 1 µCi/ml (Perkin Elmer, MA, USA) during matrix synthesis. Matrix labelling was confirmed by matrix extraction and liquid scintillation counting. After 72 h media are removed, plates washed with PBS and cells removed as described above. The soluble ECM fraction is collected and protein concentration determined using the BCA assay. Dishes are washed with PBS and the remaining ECM degraded using 1 µg/ml recombinant MMP (Biogenesis, Poole, UK) in reaction buffer (0.5 M Tris–HCl, 1.5 M NaCl, 50mM CaCl2 pH7.6). MMPs are activated by the addition of 2mM aminophenylmercuric acid (APMA) at 37°C prior to use. Serum free DMEM and APMA was used as a vehicle control, and serum free DMEM with Complete Mini Protease Inhibitor (Roche) as a negative control. Proteolysis was quantified by scintillation counting of supernatants. Fifty µls of the supernatant are removed and digested ECM determined by scintillation counting. The remaining ECM is solubilised and degradation expressed as % degradation of the total 3H proline labelled ECM.

Culture of fibroblasts on ECM substrates of variable stiffness

Tissue culture plates containing silicone gels of Young's modulus of 0.2kPa, 0.5kPa, 2kPa, 8kPa, 16kPa, 32kPa and 64kPa (SoftSubstrates, CA, USA) were used to assess the effect of ECM stiffness on TG2 activity. Six well plates of variable stiffness were coated in 100ug/ml collagen (Advanced Biomatrix, USA) overnight at room temperature. Remaining collagen solution was aspirated and cells seeded at 300,000 cells per well in serum free DMEM.

Scanning Electron Microscopy

Cell cultures were grown on glass cover slips and decellularised or imaged directly. Cultures were washed with PBS and replaced with a 3% glutaraldehyde overnight at room temperature. After washing 1% Osmium Tetroxide was added for 2 hours, washed and dehydrated in ethanol. Critical point drying using liquid CO_2 to remove any remaining moisture and they were gold coated using a sputter coater before being transferred back for imaging. Samples were imaged on a JEOL 6060LV variable pressure scanning electron microscope (Jeol Ltd, UK).

Transglutaminase Activity Assay

Transglutaminase activity was determined using the Transglutaminase Assay Kit (Sigma Aldrich) according to the manufacturers instructions.

TG2 and LOXL3 protein quantification

Human TG2 and LOXL3 ELISAs were obtained from Cloud Clone Corps. (USA) and Cusabio. Life Science (China) respectively and performed according to the manufacturer's protocols.

LOX Activity Assay

LOX activity was measured using a fluorometric assay obtained from Abcam (UK) and performed to the manufacterer's protocols with a final sample volume of 50µl supernatant.

Quantification of histological staining

Stain intensity and proliferation were analysed in 8 IPF biopsies to assess the potential correlation between the N-epsilon gamma glutamyl lysine cross-link and Ki67 positive proliferating cells. This was done in sequential sections in the same region of interest in each biopsy. The 'Fiji' version of ImageJ was used for this process[4]. In the cross link stained sections the images were colour deconvoluted using the H DAB vector with the preset RGB values. Of the three images each was split into, Image 2 was used for quantification. The mean grey value was taken for each Image 2 from all donors and converted to OD using the formula $OD = \log(\frac{maxIntensity}{meanIntensity})$. Proliferation was assessed by counting total cell number and all positive cells in each Ki67 stained section.

Ethical statement for animal use

All animal work was approved by the Animal Welfare and Ethical Review Board (AWERB) of the University of Nottingham (UK) and conducted in accordance with all terms of the Establishment, Project and Personal Licences issued by the Secretary of State for the Home Office. Consistent with all national and international law, studies were carried out as detailed in the Animal [Scientific Procedures] Act 1986 (Amended Regulations 2012) (ASPA), Animal Welfare Act 2006, Directive 2010/63/EU, the LASA guidelines and in respect to the principals of Replacement, Reduction and Refinement. Work was performed under licence number RGJ 40/3709 using the 19b3 protocol.

Animals and Husbandry

Power calculations were performed using PS version 3.1.2[5]. Previous work from the Jenkins group (University of Nottingham, UK) was used to calculate the values for α at 0.001, δ at 500, σ at 200 with a power of 0.95. This yielded a sample size of 8 for animal work with a standard deviation assumed of 200µg hydroxyproline and the difference of the group means of 500µg hydroxyproline. This enables us to study 8 pairs of subjects to be able to reject the null hypothesis that this response difference is zero with probability (power) 0.95. The Type I error probability associated with this test of this null hypothesis is 0.001.

C57BL/6 Mice were obtained from Charles River Laboratories (Wilmington, Mass. USA.) at age 6 – 8 weeks old. Animals were housed in a Specific Pathogen Free (SPF) environment in the Bio Support Unit, University of Nottingham, UK. Mice were randomly divided into a maximum of 4 mice per cage. Cages used were Techniplast GR500 Individually Vented Cages (IVC) at 21˚C and 50% humidity with environmental enrichment. Bedding consisted of Nestpak grade 5 sawdust (Datesand Ltd., UK) and Sizzle-Nest (Scanbur, Denmark). Mice were fed *ad libitum* 2018S Teklad Global 18% Protein Rodent

Diet (Harlan Laboratories, UK) with constant access to fresh, filtered water and maintained on a 12 hour light, 12 hour dark cycle. Food and bedding was sterilised by autoclaving prior to use. Following receipt of the animals, they were left in their new environment for 5 days to acclimatise before any experimental work began.

***Ex Vivo* TG2 activity in Bleomycin injured tissue**

Lung was harvested from three 8 week old C57BL/6 mice and dissected into 3mm cubes. Tissue cubes were placed into 6 well plates in serum free DMEM overnight. The following morning media was aspirated and media containing DMEM + 1% Insulin-Transferrin-Selenium (Gibco) + 100U/ml penicillin + 0.1mg/ml streptomycin (Sigma Aldrich, Dorset, UK). Bleomycin was added to non-control samples at 5ug/ml on the lung samples and 15ug/ml on liver samples. This was chosen as liver samples were approximately three times heavier per cube than lung tissue cystamine was added to a final concentration of 0.5mM to one of the non-Bleomycin treated samples and to one of the Bleomycin treated. Samples were incubated in humidified atmosphere with 5% CO_2 at 37°C for 23 hours. Cystamine was added to a further tissue sample at t+23 hours. Incubation was resumed for another hour before all media was harvested for assay. Transglutaminase activity was assayed immediately following harvest. Data were normalised per mg of tissue.

Bleomycin Model of Fibrosis

All mice were anaesthetised with 2.5% inhaled isoflurane in a stream of oxygen (AB-G), weighed and ear marked. All mice received a single oropharyngeal administration of 60 IU Bleomycin (2mg/kg) in 50ul 0.9% sterile PBS or PBS only. All mice were closely monitored for full recovery and checked for health and weight loss exceeding 25% of starting weight once daily for 7 days and thereafter as required but minimum twice weekly. Day 0-14, during the inflammation stage, mice were observed for any deterioration in health before administration of experimental cystamine.

Murine Experimental Procedures

Mice were randomly allocated to each treatment group. Following bleomycin installation mice received intraperitoneal (IP) injection of 100µl saline or cystamine once daily for 10 consecutive days during time course (TC) 1 and 11 for TC 2, starting at various time points (TP), precisely d14, d24 and d34. The day after the last IP, mice were sacrificed by terminal anaesthesia (AC) as described below. The dose of cystamine was calculated based on an average weight of bleomycin treated mice at the starting point of each IP treatment series.

Terminal Anaesthesia and sample collection

Sacrifice was conducted in accordance with ASPA Schedule 1. Avertin, or tribromoethanol, is no longer sold commercially for anaesthesia, therefore a non-pharmaceutical alternative was made under guidance of the Named Veterinary Surgeon (NVS). This was done by dissolving 5g 2,2,2-tribromoethanol (Sigma-Aldrich) in 5ml 2-methyl-2-butanol (Sigma-Aldrich) under vigorous agitation in sterile conditions. This 100% Avertin solution was stored under light protection at 4˚C. Just prior to use, a working solution was made by diluting the stock solution to 2.5% using warmed PBS. pH was assessed in every batch before use.

Terminal anaesthesia was carried out by administering 500µl of 2.5% Avertin by IP injection. This calculation is based on a 25g mouse and was adjusted accordingly per average cage weight. Induction required 1-2 minutes and mice were left for at least 5 minutes to enter deep anaesthesia

and then checked by pinching the foot and for blink reflex. Tissue was collected, weighed, and snap frozen on dry ice for protein analysis.

Supplementary Results

Fibroblast characterisation

Fibroblasts obtained from control and IPF lung resections were characterised by their adherence to plastic tissue culture plates, morphology and the expression of S100A4, FAP and αSMA. Commercial human lung fibroblasts had the same morphology and expressed the same markers as those derived from primary tissue (supplementary figure 1). Whilst airway smooth muscle cells expressed the same markers at a lower level they could be distinguished by the presence of well-developed actin stress fibers as previously described[6].

Characterisation of fibroblast derived ECM

ECM derived from normal and IPF fibroblasts was imaged by electron microscopy and was observed to coat tissue culture surfaces evenly and be free of cellular debris (supplementary figure 2a). Total ECM protein was measured in soluble and insoluble fractions. There was no significant difference in either ECM protein fraction between normal and IPF derived fibroblasts (supplementary figure 2b). Total collagen, measured using a hydroxyproline assay, was predominantly located in the insoluble fraction but did not differ between normal and IPF derived fibroblasts (supplementary figure 2c). Labelling ECM by incubating fibroblasts during ECM deposition with tritiated proline confirmed that deposition of proline labelled ECM (predominantly collagen) was also equal in normal and IPF derived fibroblasts (supplementary figure 2d).

Collagen 1-5 mRNA levels

Quantitative RT-PCR was conducted to ascertain if the matrix varied in terms of relative collagen levels expressed by the cells rather than total quantity as shown by the hydroxyproline and tritiated proline incorporation assays. Cells were cultured as previously described to passage 4, RNA extraction, cDNA synthesised and RT-PCR was conducted with ribosomal 18S as the housekeeping gene using KiCqStart SYBR Green Primers for the alpha chains of collagens 1-5 (Sigma Aldrich, Dorset, UK). Collagen type III was the most highly expressed transcript, with Collagen II being the lowest expressed relative to 18s as shown. Collagen I in control cells was expressed at low levels relative to 18S and at similar levels between cells within the group. This is in contrast to the IPF group where the standard deviation is greater than that of control (supplementary figure 3). No statistical difference was observed between the IPF and control fibroblasts (n=3).

IPF ECM does not protect against induced apoptosis

To determine if IPF derived ECM could protect fibroblasts against apoptosis: control and IPF derived fibroblasts were treated with either Fas ligand (100ng/ml) or staurosporine (1µmol) for 24 hours to induce apoptosis whilst on control or IPF derived ECM. Levels of TUNEL staining ranged between 20 to 30% in both control and IPF derived fibroblasts treated with either Fas ligand or staurosporine. Whilst IPF derived fibroblasts on fibroblast derived ECM tended to have lower levels of apoptosis, these differences, and all other combinations of cell type or matrix substrate, were not significant (supplementary figure 6). Similarly Caspase 3 and PARP cleavage assessed by western blotting under the same conditions did not differ between cell or matrix type.

Figure Legends

Supplementary figure 1. Characterisation of control and IPF derived fibroblasts. Images of stained primary human airway smooth muscle (ASM) cells (used as controls), IPF and control patient derived fibroblasts. All cells are stained with anti α-smooth muscle actin (α-SMA, red) and DAPI (blue). Green staining is used for anti-S100A4 and fibroblast activation protein (FAP-1) as indicated. Control and IPF derived fibroblasts have similar morphology and

staining patterns. ASM cells express s100A4 and FAP at a lower level than fibroblasts and have more pronounced stress fibers. Representative images are shown. For each cell type three separate donors were studied.

Supplementary figure 2. Characterisation of fibroblast derived ECM. (a) Fibroblast derived ECM preparation visualised by scanning electron microscopy showing a complex filamentous layer free from cells and debris. (b) Control and fibroblast ECM preparations analysed by BCA assay contain similar levels of total protein in their soluble and insoluble fractions. (c) Measurement of total collagen in ECM preparations show this is similar in control and IPF derived fibroblasts and largely in the insoluble fraction. (d) Equal collagen synthesis between control and IPF derived fibroblasts is confirmed by tritiated proline incorporation assay.

Supplementary figure 3. Collagen Type I-V mRNA expression does not vary between IPF and control fibroblasts. (a-e) Collagen types I-V mRNA does not vary between IPF and control fibroblasts assayed by real time PCR. Data presented ±SD, n=3.

Supplementary figure 4. Lysyl Oxidase like protein (LOXL) expression in IPF tissue. LOXL2 is expressed in control and IPF lung. LOXL3 is not present in control lung but weakly positive in IPF lung. Brown indicates positive staining; Blue indicates haematoxylin counterstaining of nuclei. Magnification x20.

Supplementary figure 5. IPF derived ECM induces LOXL3 expression. Three control and three IPF derived fibroblasts were cultured on three control and three IPF derived ECM preparations and gene expression for cross linking enzymes quantified by real time PCR. LOXL3 was strongly induced on IPF derived ECM in both cell types. TG2 shows a trend towards increased expression in IPF derived fibroblasts regardless of matrix type. LOX shows a trend towards lower expression on IPF derived ECM however neither are significant. These data are bar graphs of the same data as shown in figure 3 in the main manuscript.

Supplementary figure 6. IPF ECM does not protect against staurosporine or fas ligand induced apoptosis. Three control and three IPF derived fibroblasts were cultured on three control and three IPF derived ECM preparations and apoptosis induced by staurosporine (1µg) or fas ligand (100ng/ml) for 24 hours. (a & b) IPF matrix did not affect the percentage of TUNEL positive cells induced by either agent when compared with control ECM. (c) Western blotting of or three control and IPF derived fibroblasts cultured on control and IPF derived ECM and treated with staurosporine (1µg) or fas ligand (100ng/ml), shows no difference in cleaved PARP or caspase 3 between ECM types.

Supplementary figure 7. Serum LOXL3 and transglutaminase 2 are not elevated in patients with IPF. (a & b) Serum LOXL3 and Transglutaminase 2 (c & d) are not elevated in serum from patients with IPF or related to survival at three years or lung function.

Supplementary figure 8. ECM stiffness does not affect fibroblast transglutaminase activity. Control fibroblasts were cultured on ECM substrates with a Young's modulus of 0.5 to 64 kPa and incubated for 24 to 72 hours. ECM stiffness had no impact upon fibroblast derived transglutaminase activity.

Supplementary figure 9. Association of TG2 mediated cross-linking with proliferation. (a) Immunohistochemical staining of TG2 mediated cross-links and ki67 in fibrotic regions from eight IPF lung biopsies. Proliferating cells are identified by brown nuclear staining. (b) Quantification of TG2 staining and ki67 positive cells in eight IPF biopsies. Cell proliferation and TG2 cross-link density are not significantly related R^2=0.011

Supplementary figure 10. Tritiated hydroxyproline release from ECM during MMP mediated proteolysis. Liberation of radio-labelled collagen fragments from control and IPF derived IPF treated with vehicle, cystamine of βAPN, normalised to scintillant only background in the presence of: (a) DMEM only control (b) APMA vehicle control (c) APMA activated MMP-1 (d) MMP-2 (e) MMP-1 and -2 (f) MMP7. Data presented ±SD. DPM= disintegrations per minute. n=3.

Supplementary figure 11. Total lung hydroxyproline in the bleomycin model over time. Mice were treated with intra-tracheal saline or bleomycin at day 0 and total lung hydroxyproline measured after 24, 34 and 44 days. Bleomycin was associated with increased whole lung collagen but this did not change significantly over the period of measurement. * P<0.05, ***P<0.001, n=4.

Supplementary references

1. Markwick L, Clements D, Roberts M, Ceresa C, Knox A, Johnson S. CCR3 induced p42/44 MAPK activation protects against staurosporine induced DNA fragmentation but not apoptosis in airway smooth muscle cells. *Clinical and Experimental Allergy.* 2012;42:1040-1050.
2. Lu P, Weaver VM, Werb Z. The extracellular matrix: A dynamic niche in cancer progression. *The Journal of Cell Biology.* 2012;196(4):395-406.
3. Ngoka L. Sample prep for proteomics of breast cancer: proteomics and gene ontology reveal dramatic differences in protein solubilization preferences of radioimmunoprecipitation assay and urea lysis buffers. *Proteome Science.* 2008;6(1):30.
4. Schindelin J, Arganda-Carreras I, Frise E, et al. Fiji: an open-source platform for biological-image analysis. *Nature methods.* 2012;9(7):676-682.
5. Dupont WD, Plummer WD, Jr. Power and sample size calculations. A review and computer program. *Controlled clinical trials.* 1990;11(2):116-128.
6. Singh SR, Billington CK, Sayers I, Hall IP. Can lineage-specific markers be identified to characterize mesenchyme-derived cell populations in the human airways? *Am J Physiol Lung Cell Mol Physiol.* 2010;299(2):L169-183.